FIZ-KA--12 1988

NEANDC (E)-282 U Vol. V
INDC (Ger) - 30/LN + Special

PROGRESS REPORT ON NUCLEAR DATA RESEARCH IN THE FEDERAL REPUBLIC OF GERMANY

for the Period April 1, 1986 to March 31, 1987

FACHINFORMATIONS-
ZENTRUM
KARLSRUHE

ISSN 0172-2204

FIZ-KA--12 · Januar 1988

NEA NDC (E)-282 U Vol. V
INDC (Ger) - 30/LN + Special

PROGRESS REPORT ON NUCLEAR DATA RESEARCH IN THE FEDERAL REPUBLIC OF GERMANY

for the Period April 1, 1986 to March 31, 1987

Edited by
S. Cierjacks
Kernforschungszentrum Karlsruhe
Institut für Kernphysik

and

H. Behrens
Fachinformationszentrum Karlsruhe

Fachinformationszentrum Karlsruhe

Vertrieb:

FACHINFORMATIONS-
ZENTRUM
KARLSRUHE

7514 Eggenstein-Leopoldshafen 2
Telefon 07247/82-4600, -4601
Teletex 724710=FIZKA,
über Telex 17724710+
Telefax 07247/2968

Preis: DM 21,00 incl. Porto + MWST.

Alle Rechte vorbehalten
© Fachinformationszentrum Karlsruhe, 1988
Printed in the Federal Republic of Germany
ISSN 0172-2204

Druck: Reprodienst GmbH, Gündlinger Straße 8, 7800 Freiburg i. Br.

This document contains information of a preliminary or private nature and should be used with discretion. Its contents may not be quoted, abstracted or transmitted to libraries without the express permission of the originator.

FOREWORD

This report has been prepared to promote exchange of nuclear data research information between the Federal Republic of Germany and other member states of NEA and IAEA. It brings together progress reports from KfK Karlsruhe, KFA Jülich, GKSS-Geesthacht, the Universities of Hamburg, Köln, Mainz, Marburg, Munich and Stuttgart, as well as from PTB Braunschweig and FIZ Karlsruhe. As in previous years, the emphasis in the work reported here has been on measurement, evaluation and compilation of application oriented nuclear data, such as those relevant to fission and fusion reactor technologies, development of intense spallation neutron sources, astrophysics research, cosmogenic and meteoritic investigations, production of medically important short-lived radioisotopes, etc.

Each contribution is presented under the laboratory heading where the work was done. If the work is relevant to requests in the World Request List for Nuclear Data, WRENDA 83/84 (INDC(SEC)-88/URSF), the corresponding request identification numbers have been listed after the title and authors' names of the respective contribution.

Karlsruhe, June 1987

S. Cierjacks
H. Behrens

CONTENTS

KERNFORSCHUNGSZENTRUM KARLSRUHE
INSTITUT FÜR KERNPHYSIK II

1. Study of Low-lying T=3/2 States in ^{13}C

S. Cierjacks, G. Schmalz[1], F. Hinterberger[2], P. v.Rossen[2]

High-resolution total neutron cross sections have been studied in the region of the lowest T=3/2 states in ^{13}C [1]. The first T=3/2 state was observed as a weak resonance anomaly at 15108.2 ± 1.2 keV excitation. The deduced resonance parameters agreed with previous results obtained from charged-particle work. At higher excitation energies four narrow resonance anomalies were found at 17533 ± 3, 18082 ± 3, 20057 ± 4 and 21704 ± 4 keV. Possible T=3/2 assignments for the latter four resonances have been examined. A typical result from our work is shown in Fig. 1 which contains the information for the narrow resonance anomaly around 17533 keV. Finally, an upper limit of the elasticity parameter, $(J+1/2)\ \Gamma_{no}/\Gamma$, was deduced from transmission data for those T=3/2 states which did not appear as significant resonance anomalies.

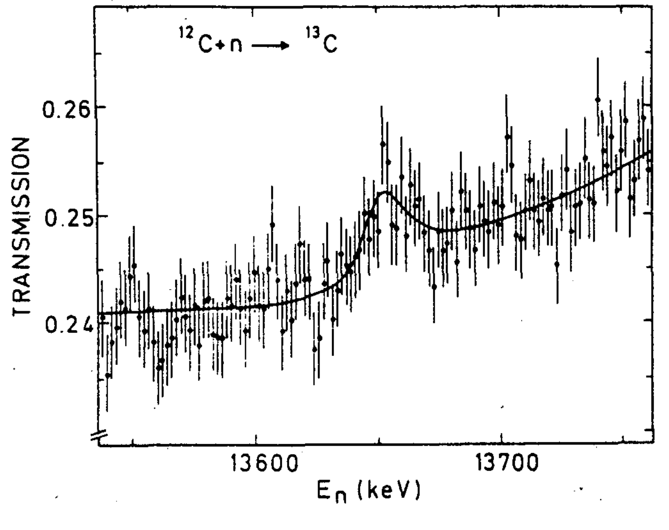

Fig. 1 The C + n transmission in the ^{13}C excitation region around E_x=17533 keV. The solid line results from a nonlinear least-squares fit of seven resonance parameters.

2. Measurements of Differential Neutron Production Cross Sections for Protons of 585 MeV Incident on Targets with $12 \leq A \leq 238$

S. Cierjacks, Y. Hino[3], F. Raupp[1], L. Buth [4], D. Filges[5], P. Cloth[5], T.W. Armstrong[5]

In continuation of our previous work a final journal publication of the experimental data has been completed [2]. The publication summarizes double differential neutron production cross sections for C, Al, Fe, Nb, In, Ta, Pb and U targets at emission angles of 30°, 90° and 150° and for secondary neutron energies between 0.9 and 585 MeV. The experimental data all reveal a clear two-component structure with contributions from intranuclear cascade reactions and from subsequent evaporation processes in highly excited compound nuclei. For heavy and medium weight nuclei the data in the evaporation region are indicative of an isotropic angular distribution in the zero linear momentum coordinate system. Data in the cascade region are strongly peaked in the forward direction as expected from theory. The fraction of cascade neutrons increases rapidly with decreasing emission angle and smoothly with decreasing target mass number. The results of our measurements have been compared with previous determinations of neutron and proton production cross sections from other laboratories.

3. HETC Calculations of Differential Neutron Production Cross Sections for High-Energy Protons on Targets with $12 \leq A \leq 238$

D. Filges[5], P. Cloth[5], T.W. Armstrong[5], S. Cierjacks, Y. Hino[3], F. Raupp[1], L. Buth[4]

Extended calculations of differential neutron production cross sections and secondary particle yields for high-energy protons have been finalized [3]. The calculations are based on the intranuclear cascade-evaporation model with important changes of model parameters used in the standard version of the HETC. The corresponding changes were justified by detailed comparisons of predictions with a large variety of new experimental results measured in recent spallation-source studies. They resulted in a new code version called HETC/KFA-1. The calculations have been compared with our systematic measurements of differential neutron production cross sections (see Sect. 2). In general the code predicts approximately the correct neutron production in the evaporation region, whereas in the cascade region ($E_n \geq 20$ MeV) systematic discrepancies are found. These increase rapidly with increasing neutron energy and increasing emission angle. In Fig. 2 the calculated and measured 90° neutron production cross sections for 585 MeV protons are compared. It can be seen that there is good agreement over the whole evaporation region, even for the lightest target elements, carbon and aluminum. However, above ~20 MeV the HETC/KFA-1 still underpredicts systematically the measurements. At maximum energy around 500 MeV the calculations differ by more than a factor of 10.

4. Neutron Fission Cross Sections of ^{235}U, ^{239}Pu and ^{240}Pu and Fission Cross Section Ratios of $^{239}Pu/^{235}U$ and $^{240}Pu/^{235}U$

S. Cierjacks

Work has been started to complete or reanalyse previously determined neutron fission cross sections or cross section ratios [4,5,6]. Especially data given in Ref. 5 were previously only analyzed in preliminary form: For the absolute fission cross sections of ^{235}U only approximate detection efficiencies of our special proton recoil detectors have been used, because final efficiencies were not yet available at that time. In addition, shape measurements of $^{238}U/^{235}U$ and $^{239}Pu/^{235}U$ in Ref. 4 were normalized arbitrarily at 14 MeV due to the lack of final mass determinations. Concerning the fission cross sections of ^{239}Pu and the fission cross section ratios of $^{239}Pu/^{235}U$ determined in the work of Ref. 6 doubts about the accuracy of the energy scale have been raised in a recent ENDL evaluation [7]. To investigate this problem, a reanalysis of the corresponding raw data has been started. After completion of the evaluational work a final journal publication of all neutron fission measurements with the KfK cyclotron is foreseen.

---

[1] Kernforschungszentrum Karlsruhe, Institut für Kernphysik I

[2] Institut für Strahlen- und Kernphysik, Universität Bonn

[3] Now at Electrotechnical Laboratory, 114 Umezono, Ibaraki, Japan

[4] Kernforschungszentrum Karlsruhe, Institut für Neutronenphysik und Reaktortechnik

[5] Institut für Reaktorentwicklung, Kernforschungsanlage Jülich

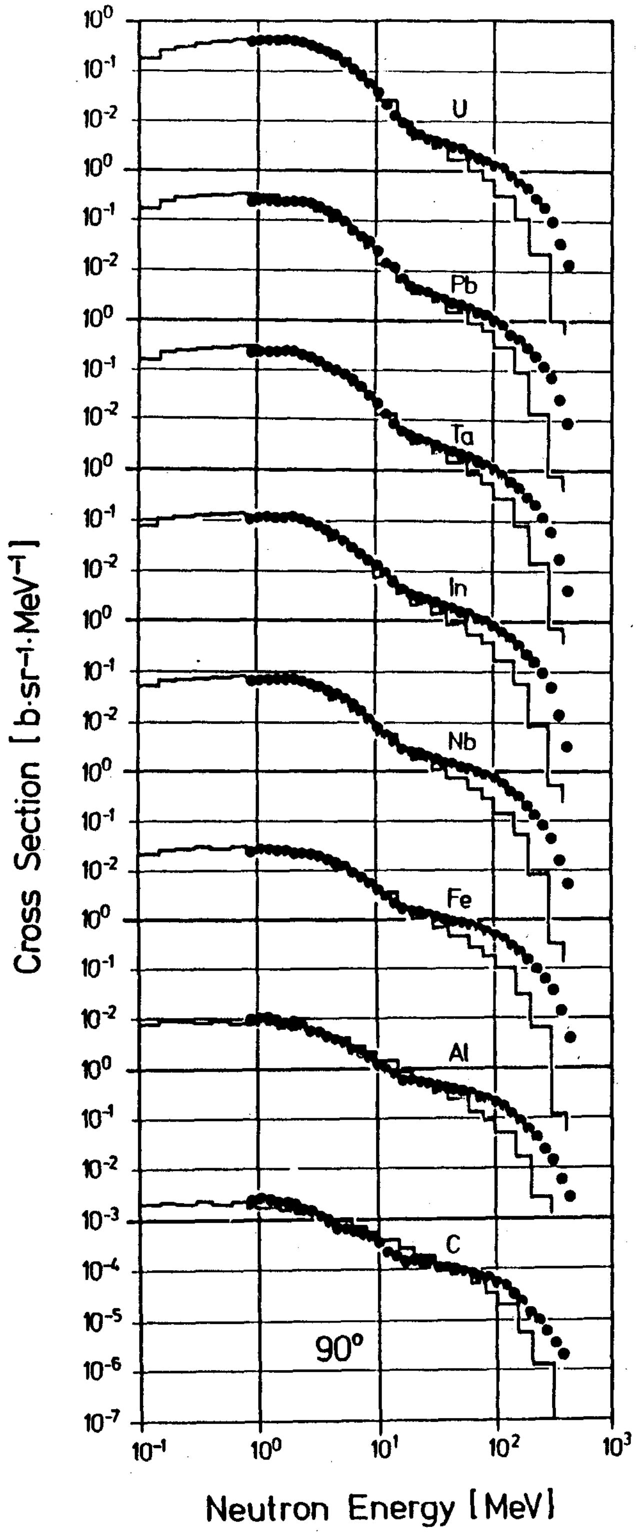

Fig. 2 Comparison of measured and calculated neutron production cross sections for eight specified target elements at 90° emission angle and 585 MeV incident proton energy. Full circles represent measured data points; The solid line histograms show the results of HETC/KFA-1 calculations.

References

[1] F. Hinterberger, P. v.Rossen, S. Cierjacks and G. Schmalz; High resolution study of the ^{12}C+n total cross section in the region of ^{13}C T=3/2 states; Z. Phys. A326(1987)407

[2] S. Cierjacks, Y. Hino, F. Raupp, L. Buth, D. Filges, P. Cloth and T.W. Armstrong; Systematics of angular-dependent neutron production by 585 MeV protons on targets with 12 ≤ A ≤ 238: Differential cross section measurement; Phys. Rev. C (in press)

[3] D. Filges, P. Cloth, T.W. Armstrong, S. Cierjacks, Y. Hino, and L. Buth; Systematics of angular-dependent neutron production by 585 MeV protons on targets with 12 ≤ A ≤ 238: Validation of intranuclear cascade-evaporation model calculations; Phys. Rev. C (in press)

[4] B. Leugers, S. Cierjacks, P. Brotz, D. Erbe, D. Gröschel, G. Schmalz and F. Voss; The ^{235}U and the ^{238}U neutron-induced fission cross sections relative to the H(n,p) cross section; Argonne National Laboratory Report, ANL-78-90, 1976, p. 246

[5] S. Cierjacks, B. Leugers, K. Kari, P. Brotz, D. Erbe, D. Gröschel, G. Schmalz and F. Voss; Measurements of neutron-induced fission cross section ratios at the Karlsruhe isochronous cyclotron; Argonne National Laboratory Report, ANL-78-90, 1976, p. 94

[6] K. Kari; Messung der Spaltquerschnitte von ^{239}Pu und ^{240}Pu relativ zum Spaltquerschnitt von ^{235}U und zum Streuquerschnitt H(n,p) im Neutronenenergiebereich zwischen 0.5 und 20 MeV; Kernforschungszentrum Karlsruhe Report, KfK 2673, 1978; and K. Kari and S. Cierjacks; Measurements of the fast fission cross sections of ^{239}Pu and ^{240}Pu; Proc. Int. Conf. on Neutron Physics and Nuclear Data, Harwell 1978, p. 905

[7] R.J. Howerton and R.M. White; A reevaluation for ENDL of $\sigma(n,f)$ and ν_p for ^{235}U and ^{239}Pu from 100 keV to 20 MeV; Lawrence Livermore National Laboratory Report, UCID-19973, 1984

KERNFORSCHUNGSZENTRUM KARLSRUHE
INSTITUT FÜR KERNPHYSIK III

1. Stellar Krypton Cross Sections at kT = 25 and 52 keV*

F. Käppeler, A.A. Naqvi +, M. Al-Ohali +

Studies of neutron capture nucleosynthesis in the s-process usually refer to a thermal energy of kT = 30 keV, corresponding to a temperature of T = 3.5 10^8 K. This convention is justified as stellar neutron capture rates are in general not sensitive to temperature due to the approximate $(E_n)^{-1/2}$-dependence of most capture cross sections. But several important exceptions from this rule require more detailed information on the variation of the average stellar cross section with temperature. We show that activation measurements can be performed in a quasi stellar neutron spectrum for kT = 52 keV, using kinematically collimated neutrons from the ^{3}H(p,n) reaction. Neutron capture cross sections were measured in this spectrum and at kT = 25 keV for ^{86}Kr(n,γ) and for the reaction ^{84}Kr(n,γ)^{85m}Kr, which populates the isomeric state in ^{85}Kr. In this way, the respective 30 keV cross sections of 3.5 ± 0.3 mb and 16.7 ± 1.2 mb could be derived by interpolation.

* Phys. Rev. C35 (1987) 936

\+ University of Petroleum and Minerals, Dhahran, Saudi Arabia

2. Measurement of the ^{85,87}Rb Capture Cross Sections for s-Process Studies

H. Beer, R.L. Macklin +

Neutron capture cross section measurements have been carried out for the isotopes ^{85,87}Rb in the energy range 2.6 to 500 keV. Resonance parameters for the observed resonances were determined by a shape analysis. Fig. 1 shows the resonances around 30 keV neutron energy. Maxwellian average capture cross sections were computed for thermal energies kT between 5 and 100 keV. The results were used to study the s-process branching at ^{85}Kr in the frame of the pulsed model.

\+ Oak Ridge National Laboratory

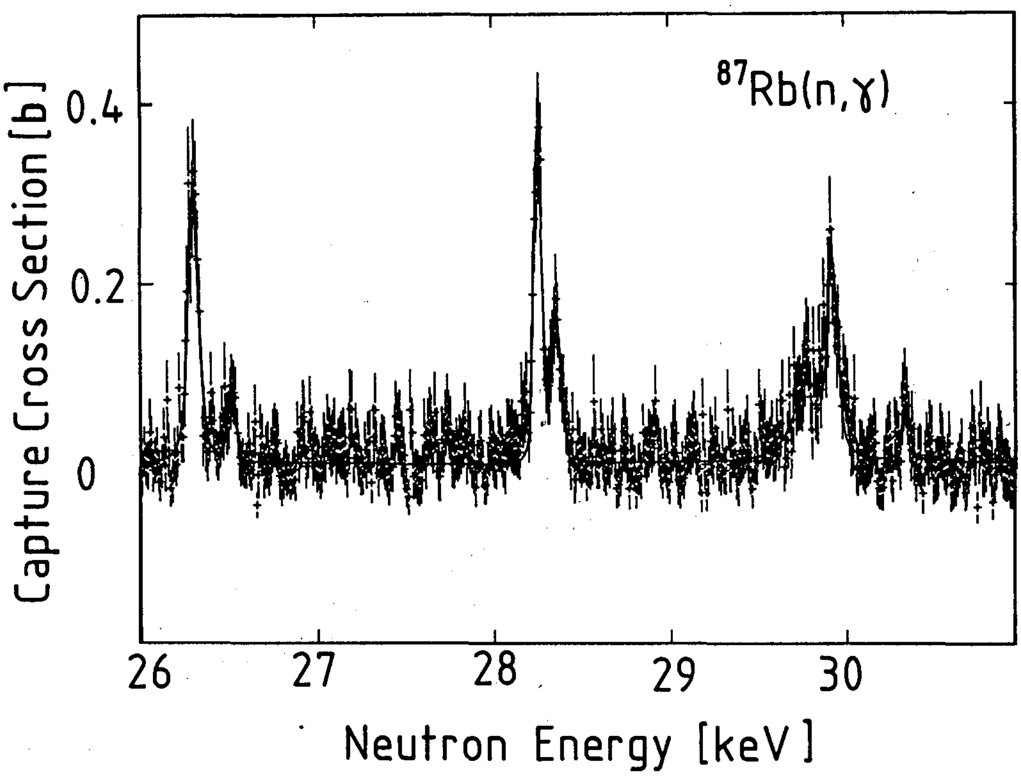

Fig. 1 ^{87}Rb(n,γ) yield data. The solid line is generated from the least squares fitting code.

3. The ^{151}Sm Branching, a Probe for the Irradiation Time Scale of the s-Process

H. Beer, R.L. Macklin+

The excitation functions for the reactions ^{152,154,155,157}Gd(n,γ) have been measured over the neutron energy range of 3 keV to 500 keV. In Fig. 1 the capture cross sections for ^{152,154}Gd are shown. Maxwellian averaged capture cross sections for thermal energies kT = 5-100 keV have been calculated. At kT = 30 keV we have found: $\sigma(^{152}Gd) = 1003 \pm 30$ mb, $\sigma(^{154}Gd) = 878 \pm 27$ mb, $\sigma(^{154}Gd) = 2721 \pm 90$ mb, $\sigma(^{157}Gd) = 1355 \pm 39$ mb. The data, in conjunction with other cross sections and solar abundances, were used to carry out an s-process analysis of the branchings in the Sm to Gd mass range. The s-process is treated in the classical as well as in the pulsed mode. The solution of the classical model is contained in the pulsed model as the asymtotic solution for large pulse widths. It is shown that this solution is the only one which can reproduce the abundance pattern of the different branchings. Pulse durations are limited to values larger than about 3 yr.

\+ Oak Ridge National Laboratory

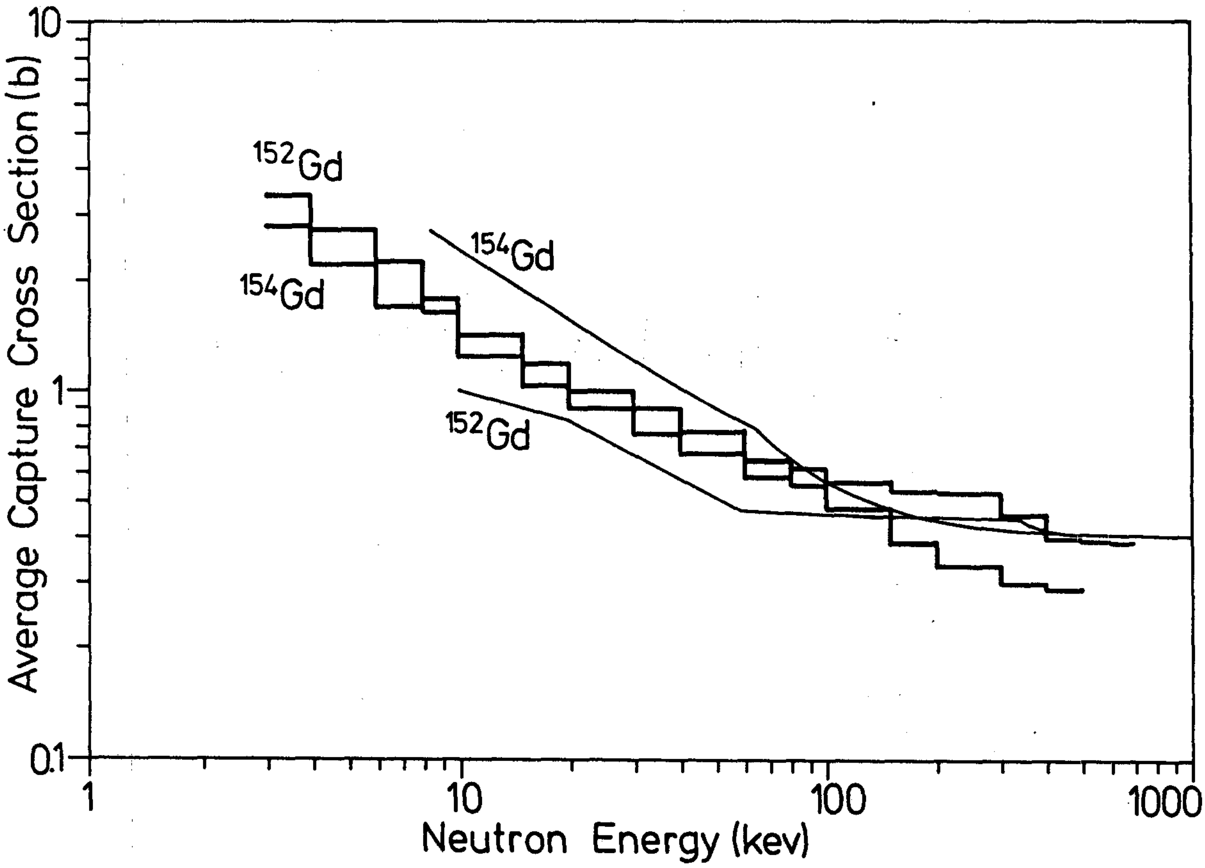

Fig. 1 Effective cross sections of $^{152,154}Gd(n,\gamma)$ as a function of neutron energy. Solid lines are theoretical estimates.

4. The Stellar Capture Cross Section of ^{197}Au - An Absolute Measurement at kT = 25 keV

W. Ratynski+, F. Käppeler

Gold has become an important standard for neutron cross section measurements in the keV energy range, because direct neutron flux determination is very difficult in this energy domain. The advantageous features of gold are:

- only one stable isotope;
- reasonably large cross section;
- easily available with high purity;
- chemically stable;
- can be used in activation measurements.

However, the absolute magnitude of this cross section is still not sufficiently well known, various recent measurements show discrepancies of ~ 7 % for the stellar cross section at kT = 30 keV [1].

Therefore, we have started a new measurement, using the $^{7}Li(p,n)^{7}Be$ reaction for neutron production. This reaction does not only provide the time-integrated neutron flux via the ^{7}Be activity of the target, but also allows for the simulation of a Maxwellian energy spectrum at kT = 25 keV. As this spectrum is emitted in a forward cone of 120° opening angle [2], the cross section can be measured in good geometry and independent of any other standard [3,4]. Then, the extrapolation to kT = 30 keV can be made reliably as the relative energy dependence of the cross section is well known.

So far, we have started with a series of activations to systematically study the required corrections (e.g. for neutron scattering and for ^{7}Be losses from the target) and the associated uncertainties. In the final results we aim for a precision of 2 %.

1 Z.Y. Bao, F. Käppeler, Atomic Data and Nuclear Data Tables (in print)
2 H. Beer, F. Käppeler, Phys. Rev. C21 (1980) 534
3 W.P. Poenitz, J. Nucl. Energy 20 (1066) 825
4 S. Zhu, S. Jiang, Y. Chen, D. Luo, Chin. J. Nucl. Phys. 6 (1984) 23

\+ On leave from Institute for Nuclear Studies, Swierk, Poland.

5. Neutron Capture Cross Sections for s-Process Studies*

Z.Y. Bao+, F. Käppeler

The existing information on experimental and calculated neutron capture cross sections in the keV energy range was surveyed, properly renormalized if necessary, and converted into Maxwellian averages over stellar neutron spectra characterized by thermal energies between 10 and 50 keV. This compilation includes all isotopes involved in the slow neutron capture process (s-process) of nucleosynthesis between ^{12}C and ^{209}Bi as well as the longer-lived actinide isotopes which might have been modified by the s-process. Gaps in the experimental data were covered with calculated cross sections, which are particularly important in case of radioactive nuclei and for estimating the effect of thermally populated excited states. From the entire body of evaluated data a present best set of cross sections is recommended for use in s-process studies.

Of the 240 considered isotopes on or near the s-process path, Fig. 1 shows the cross sections of the odd Z nuclei. Note that most of the small cross sections near magic neutron numbers are meanwhile measured with reasonable accuracy.

* Atomic Data and Nuclear Data Tables (in print)

\+ On leave from the Institute of Atomic Energy, Academia Sinica, Beijing, Peoples Rep. of China

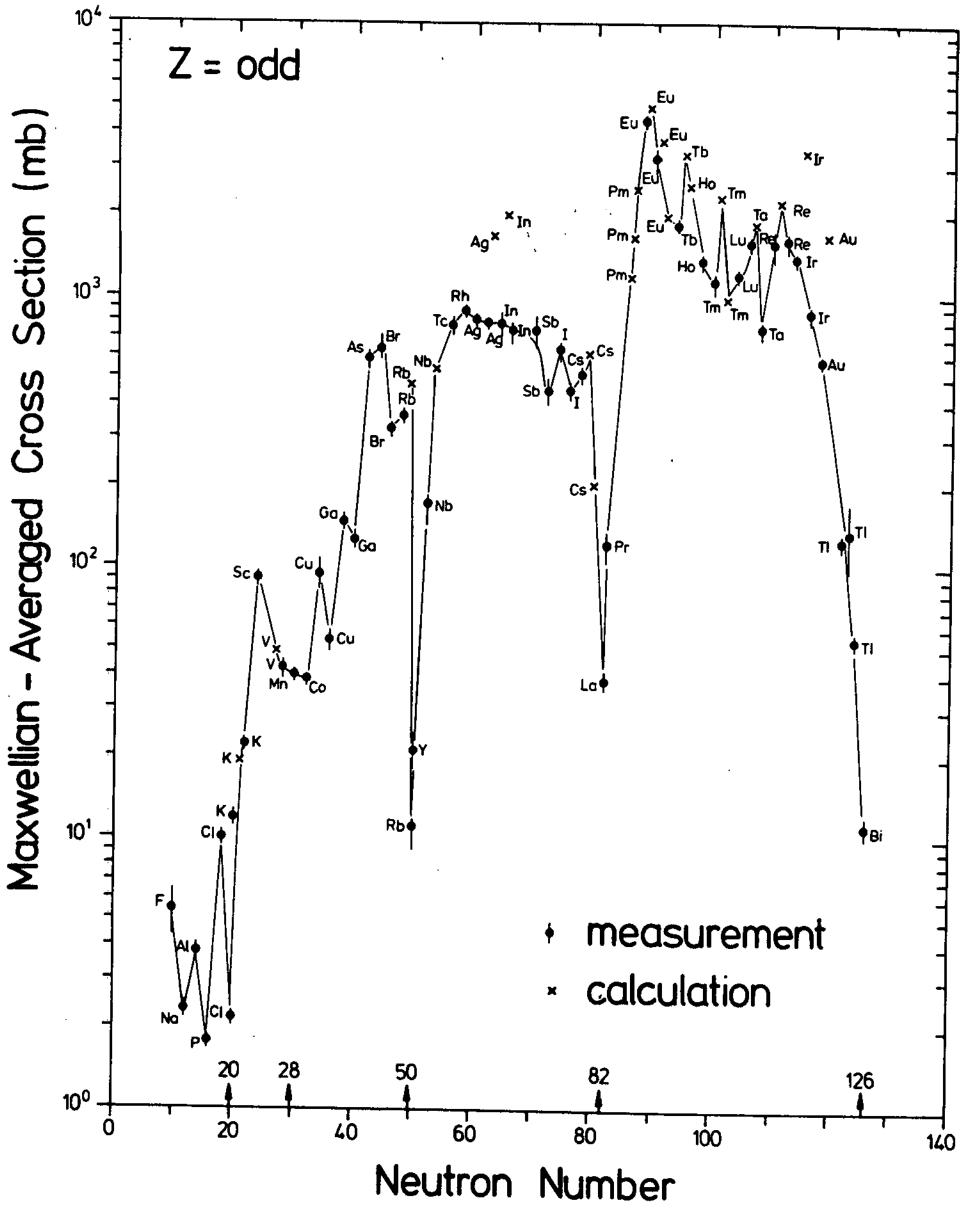

Fig. 1
Maxwellian averaged cross sections for kT = 30 keV (odd Z isotopes)

KERNFORSCHUNGSZENTRUM KARLSRUHE
INSTITUT FÜR NEUTRONENPHYSIK UND REAKTORTECHNIK

1. Nuclear data Evaluation

1.1 Evaluation of Neutron Cross Sections for ^{238}U in the Unresolved Resonance Region

F.H. Fröhner

A joint JEF-2 evaluation effort for ^{238}U+n is underway at Harwell and Karlsruhe. At KfK the unresolved resonance region between about 10 and 500 keV has been studied extensively with the Hauser-Feshbach program FITACS. This program permits coherent, simultaneous fitting of average total, capture and inelastic scattering cross sections by adjustment of strength functions, distant-level parameters and average radiation widths for all s-, p-, d- and f-wave channels. Width fluctuation corrections, so far calculated by the usual Dresner integral approximation with Moldauer's prescription for the degrees of freedom [1], are now computed rigorously via the GOE triple integral of Verbaarschot, Weidenmüller and Zirnbauer [2] in a new version of the code. Figs. 1-3 show, as an example, a simultaneous fit to recent data. From such fits it appears that the ratio of s-wave radiation width, 23.5 ± 0.3 meV, to mean level spacing, 21.5 ± 1.5 eV, inferred from resolved resonance parameters, is several percent too high in view of the average cross section data. It will be interesting to see whether the new resonance parameter set being established at Harwell will yield a higher estimate of the mean level spacing.

References

[1] P.A. Moldauer, Nucl. Phys. A344 (1980) 185

[2] J.M. Verbaarschot, H.A. Weidenmüller and M.R. Zirnbauer, Phys. Reports 129 (1985) 367;
J.M. Verbaarschot, Ann. Phys. 168 (1986) 368

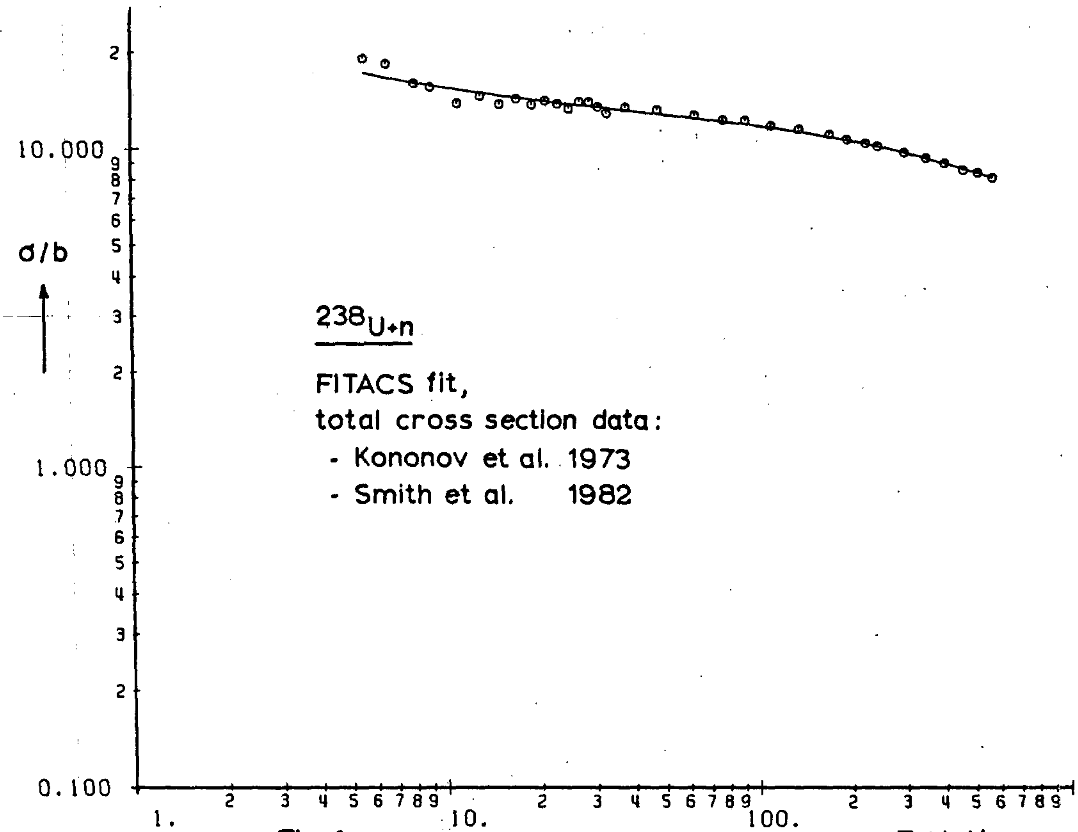

2
10.000
σ/b
1.000
0.100
^{238}U+n
FITACS fit,
total cross section data:
- Kononov et al. 1973
- Smith et al. 1982
1.
10.
100.
E / keV

Fig. 1

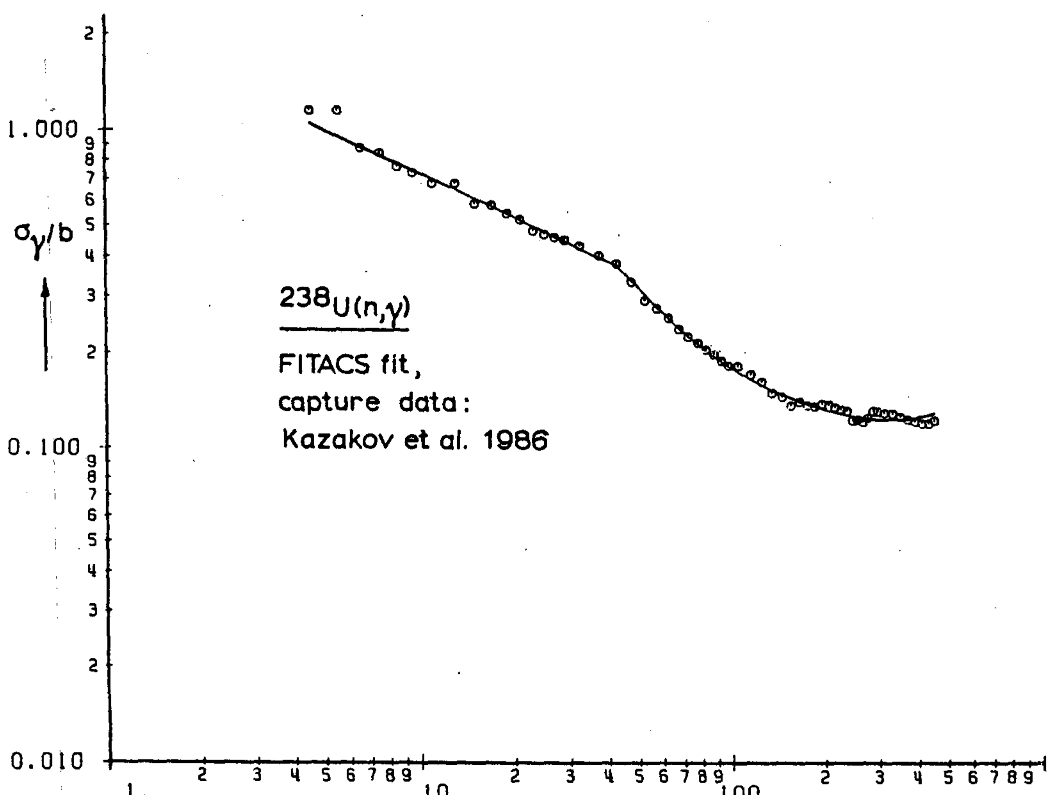

2
1.000
σγ/b
0.100
0.010
^{238}U(n,γ)
FITACS fit,
capture data:
Kazakov et al. 1986
1.
10.
100.
E / keV

Fig. 2

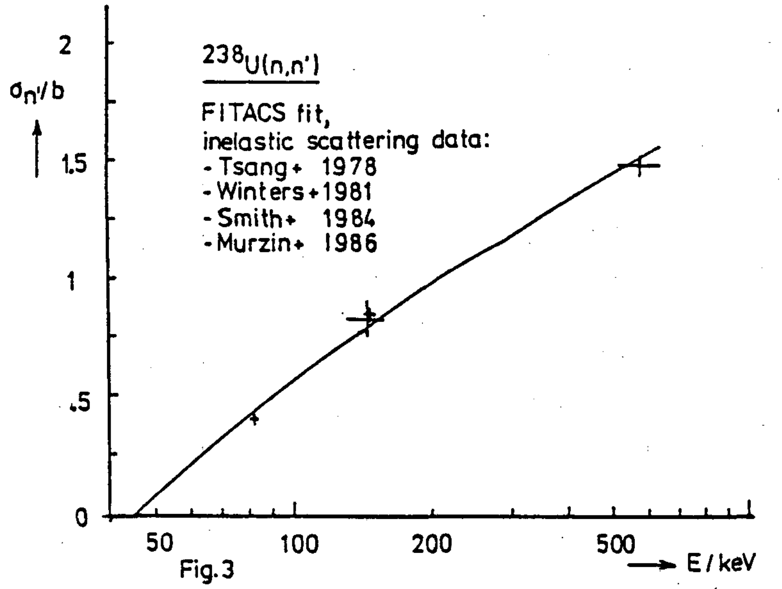

Fig.3

1.2 Evaluation of Neutron Cross Sections of ^{242}Am in the Resolved Resonance Region

F.H. Fröhner

A new evaluation of ^{242m}Am in the thermal and resolved resonance range was finished, based on the fission cross section data published by Dabbs et al. (ORNL, 1983) and on the resonance parameters for the first 48 levels by Browne et al. (LLNL, 1984), and on their thermal values and resonance parameters. The recommended thermal cross sections (2200 m/s) are 6800 b for fission, 1400 b for radiative capture and 10 b for elastic scattering. The LLNL resonance parameters were modified so as to achieve a compromise between the LLNL and ORNL data (the latter being 10 to 20 % higher).

1.3 Burnup Testing of JEF-1 Data

A. Mateeva, H.W. Wiese, U. Fischer, C. Broeders, H. Küsters

Burnup calculations for testing JEF-1 results against post-irradiation data from PWRs were made with the code KARBUS. Group constants for 69 groups were produced with a modified version of NJOY from 113 JEF materials including 20 actinides, 87 fission products, O and H (in water). Scattering matrices for water were generated for eight temperatures in cooperation with IKE, Stuttgart. Results are being compared with earlier KEDAK calculations.

1.4 Development Work on Group Constant Codes

I. Broeders, B. Krieg

The group constant code NJOY (from LANL) was modified and extended as follows. The present KfK version can cope with resonances having the unphysical (average) compound spin 1/2. A new reading routine for File 6 was written. Neutron emission cross sections (MT=10) can be processed. Group cross sections for neutron absorption are calculated. Input data are printed automatically, and calculations are not interrupted if a data type is missing. The scattering law for transfer matrices accounting for inelastic scattering, (n,2n) and (n,3n) reactions is printed out. A program, JOYFOR, was developped for translation of NJOY results in MATXS format to the KfK MITRA input format [1].

References

[1] B. Krieg and I. Broeders, "A Program for Transformation of NJOY Results in MATXS Format to the MITRA Input Format", KfK 4179 (1987)

1.5 Principles and Methods of Data Evaluation

F.H. Fröhner

The probabilistic foundations of data evaluation were reviewed for an Ispra Course on Data Uncertainty, Sensitivities, Consistency and Adjustment [1, 2]. Special attention was given to parameter estimation based on Bayes' theorem and on modern methods for the assignment of prior probabilities. The process leading from raw data to evaluated files was outlined for the case of nuclear reaction cross sections, with a discussion of the generalised least-squares principle involving prior information and nonlinear theoretical models, and of statistical and systematic errors and their propagation. It was shown how data covariances can be established from error information supplied by experimentalists, and how correlated uncertainties given in covariance files are utilised in sensitivity studies and accuracy assessments. The problem of inconsistent data was also addressed. Straightforward Bayesian two-stage estimation of unknown statistical errors leads to expressions which are similar to, but better than, the widely advertised James-Stein estimators based on educated guesswork [2].

References

[1] F.H. Fröhner, Report KfK 4099 (1986)

[2] F.H. Fröhner, "Principles and Methods of Data Evaluation", in Data Uncertainty, Sensitivities, Consistency and Adjustment, H. Rief, Y. Yeivin (eds.), Reidel, Dordrecht (in print)

1.6 On the Fusion of Polarised Deuterons

B. Goel

The reaction D + ^{3}He $\longrightarrow$ α + p can make the fusion energy production free of neutrons. The obstacles on its way are: its higher threshold compared to the currently favoured DT-fusion, scarcity of ^3He and the parasitic DD fusion which produces neutrons and radioactive tritons. Recent development; high temperature superconductors and the presence of ^3He in lunar sands require a reevaluation of the fusion cross section of the polarised deuterons.

In the case of DT-fusion it is clear that polarisation would modify the cross section substantially [1,2]. In the case of the DD-reaction it is not so. Firstly the process is more complicated than DT as 3 resonances are involved. Secondly theoretical prediction using different models contradict each other. The R-matrix [3,4] and the resonating group model (RGM) [5,6] calculations do not indicate any reduction in the cross section because of polarisation whereas DWBA calculations [7] predict a reduction to 8 - 15 % of its original value if all deuterons are polarised with parallel spins. Zhang, Liu and Shuy [7] in their latest paper show a better matching of the total cross section to the measured value as an indication of correctness of their findings. However, an examination of the equation 1 and 2 of their paper shows that the total and polarised cross section are determined by different potentials. Thus the correctness of total cross section would not imply the validity of other findings. The additive nature of different cross sections in equation 1 is questionable.

It is concluded that until further experimental or theoretical proof is available one can not count on neutron-lean D-^3He fusion by polarising deuterons.

References

[1] R.M. Kulsrud, E.J. Valeo and S.C. Cowley; Nucl. Fus. 26 (1986) 443

[2] B. Goel and W. Heeringa, Proc. of the 4th Int. Conf. on Emerging Nuclear Systems, June 30 - July 4, 1986 Madrid, p. 412

[3] G.M. Hale, Proc. of the Fusion Fuel Workshop, Madison, 20 - 30 March 1983, p. 11

[4] G.M. Hale, LA-10689-PR, Los Alamos 1985

[5] H.M. Hofmann and D. Fick, Phys. Rev. Lett. 52 (1984) 2038

[6] H.M. Hofmann, G.M. Hale, R. Wölker, Private communication 1986

[7] J.S. Zhang, K.F. Liu and G.W. Shuy, Phys. Rev. Lett. 57 (1986) 1410

INSTITUT FÜR CHEMIE (1): NUKLEARCHEMIE
KERNFORSCHUNGSANLAGE JÜLICH

1. Neutron Data

1.1 Fundamental Studies on Complex Particle Emission Reactions

S.M. Qaim, R. Wölfle

In continuation of our radiochemical studies on fast neutron induced complex particle emission reactions [cf. 1] we measured in collaboration with CBNM Geel (H. Liskien, R. Widera) the excitation function of the $^{139}La(n,t)^{137}Ba$ reaction over the neutron energy range of 16 to 19 MeV. As expected the cross sections are low (μb region). Detailed Hauser-Feshbach calculations on the first-chance emission of a triton show that the contribution of statistical processes is small.

Measurements on the $^{92}Mo(n,d)^{91m}Nb$ reaction were initiated. First results near the threshold (~ 10 MeV) show that the cross section is small. Theoretical calculations using the precompound model have been started in collaboration with IRK Vienna (H. Vonach, B. Strohmaier).

1.2 Cross Section Data Relevant to Activation Problem and Fusion Reactor Technology

R. Wölfle, A. Suhaimi, A. Mannan, S.M. Qaim, G. Stöcklin

(Relevant to request identification numbers: 724008F, 724049F, 762246F, 781211F, 781220F, 801238F, 832045F)

Triton emission cross sections in the interactions of fast neutrons with light nuclei ^{7}Li, ^{9}Be, ^{10}B and ^{14}N were determined. Measurements on the $^{7}Li(n,n't)^{4}He$ reaction were performed in the incident neutron energy range of 7.9 to 10.5 MeV [2]. The data are shown in Fig. 1 together with all the other data obtained via tritium counting. Evidently, there is a fairly good agreement between the various data. The discrepancy had arisen because of a combination of tritium and neutron emission data. This discrepancy seems to have been now removed.

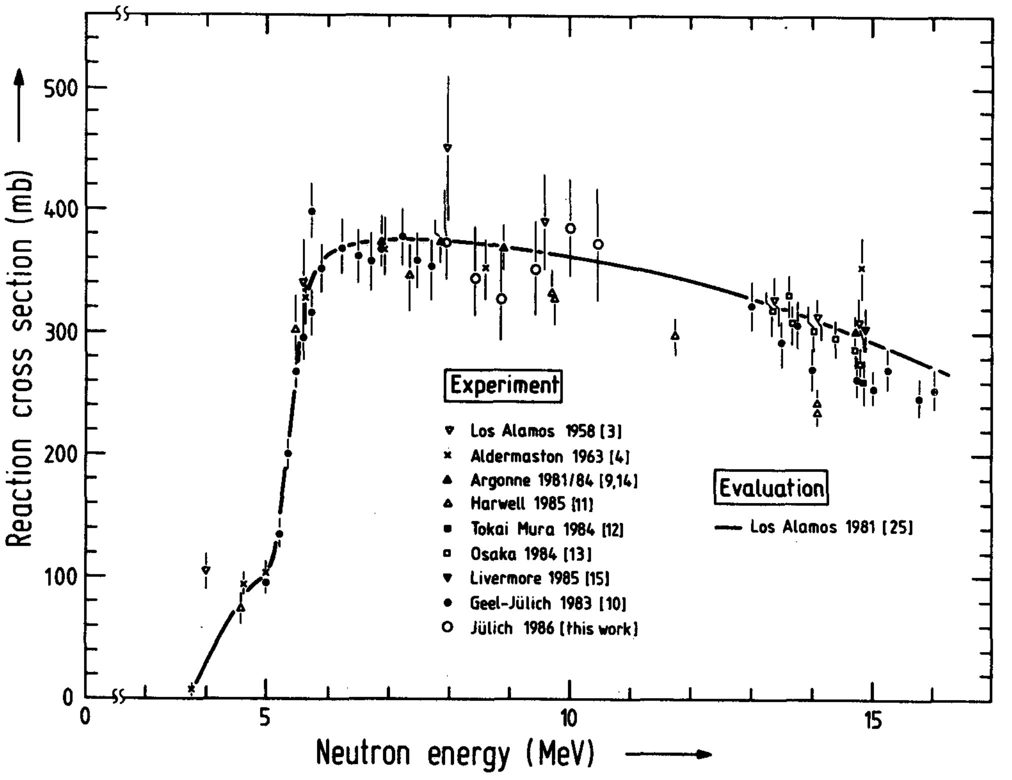

Fig. 1 Excitation function of $^{7}Li(n,n't)^{4}He$ reaction determined via tritium counting [cf. 2].

Measurements on the $^{10}B(n,t)2\alpha$ process up to E_n = 10.6 MeV were completed. The results were found to be consistent and have been reported [3]. Similar studies are also underway on the $^{14}N(n,t)^{12}C$ reaction and will be performed up to 10.6 MeV, i.e. below the threshold of the $^{14}N(n,t)3\alpha$ process.

Investigations on the $^{9}Be(n,t)^{7}Li$ reaction initiated last year with CBNM Geel (H. Liskien, R. Widera) in the energy range of 13 to 20 MeV have now been completed. The results describe the first experimentally determined excitation function for this reaction and a detailed report has been written [4].

In continuation of radiochemical studies on activation cross sections [cf. 5] we measured the $^{93}Nb(n,\alpha)^{90m,g}Y$ cross sections and isomeric cross section ratios for the first time as a function of neutron energy up to 10.6 MeV. Furthermore, excitation functions were measured over the neutron energy range of 13 to 20 MeV in collaboration with CBNM Geel (H. Liskien, R. Widera) for the reactions $^{93}Nb(n,\alpha)^{90m,g}Y$, $^{139}La(n,\alpha)^{136}Cs$ and $^{181}Ta(n,p)^{181}Hf$. All the three reactions serve as good monitors.

2. Charged Particle Data for Radioisotope Production

F. Tarkanyi, A. Mushtaq, S.M. Qaim, G. Stöcklin

In continuation of our studies [cf. 6] on the production of medically important short-lived β^+-emitting radioisotopes excitation functions were measured for $^{nat}Ge(^3He,xn)^{72,73,75}Se$ and $^{nat}Ge(\alpha,xn)^{72,73,75}Se$ processes. The data for the formation of ^{73}Se in ^3He-induced reactions are shown in Fig. 2. The results are in agreement with those of Nozaki et al. The data of Guillaume et al, if normalized to the case of ^{nat}Ge, agree in magnitude but are shifted to higher energies by about 5 MeV. According to our measurements the optimum energy range for the production of ^{73}Se is E_{3He} = 36 → 12 MeV. The thick target yield of ^{73}Se amounts to 1 mCi/μAh and the contributions of ^{72}Se and ^{75}Se impurities to 2 and 0.25 %, respectively.

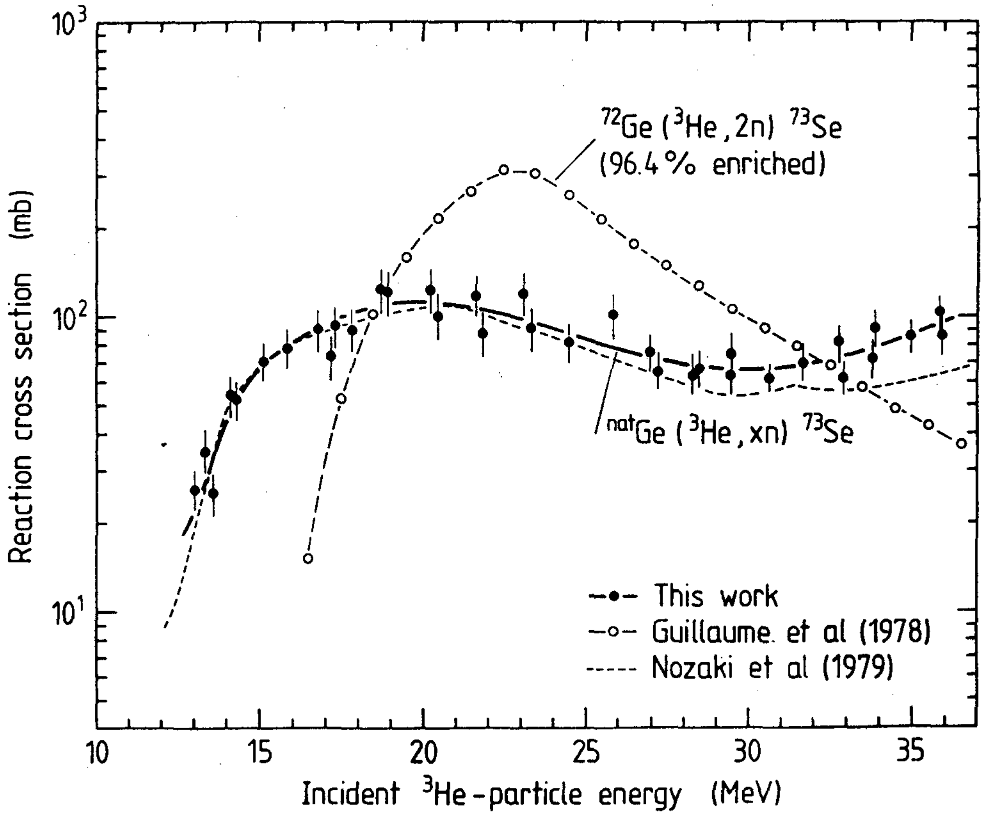

Fig. 2 Excitation functions of ^3He-particle induced nuclear reactions on ^{nat}Ge leading to the formation of ^{73}Se.

The ^{82}Sr(25d) → ^{82}Rb(1.3 min) generator system is used very widely for myocardial perfusion studies via positron emission tomography (PET). The long-lived parent is produced via spallation of Mo with 800 MeV protons. We found it worthwhile to investigate its formation at a medium-sized cyclotron using ^3He-induced reactions on Kr. For this purpose several cylinders filled with krypton at 3 bars were irradiated and the strontium activities formed were radiochemically separated and measured via γ-ray spectrometry. The results for the $^{nat}Kr(^{3}He,xn)^{82,83,85}Sr$ reactions are given in Fig. 3. The optimum energy range for the production of ^{82}Sr at a compact cyclotron is E_{3He} = 36 → 18 MeV and the thick target yield amounts to 3 µCi/µAh. If 80 % enriched ^{82}Kr could be used the yield would increase to about 20 µCi/µAh. A 30 h irradiation at a beam current of about 20 µA would lead to about 20 mCi ^{82}Sr. The reaction investigated here is thus in principle feasible for production. However, because of long irradiation times needed, it is technically difficult and possibly uneconomical.

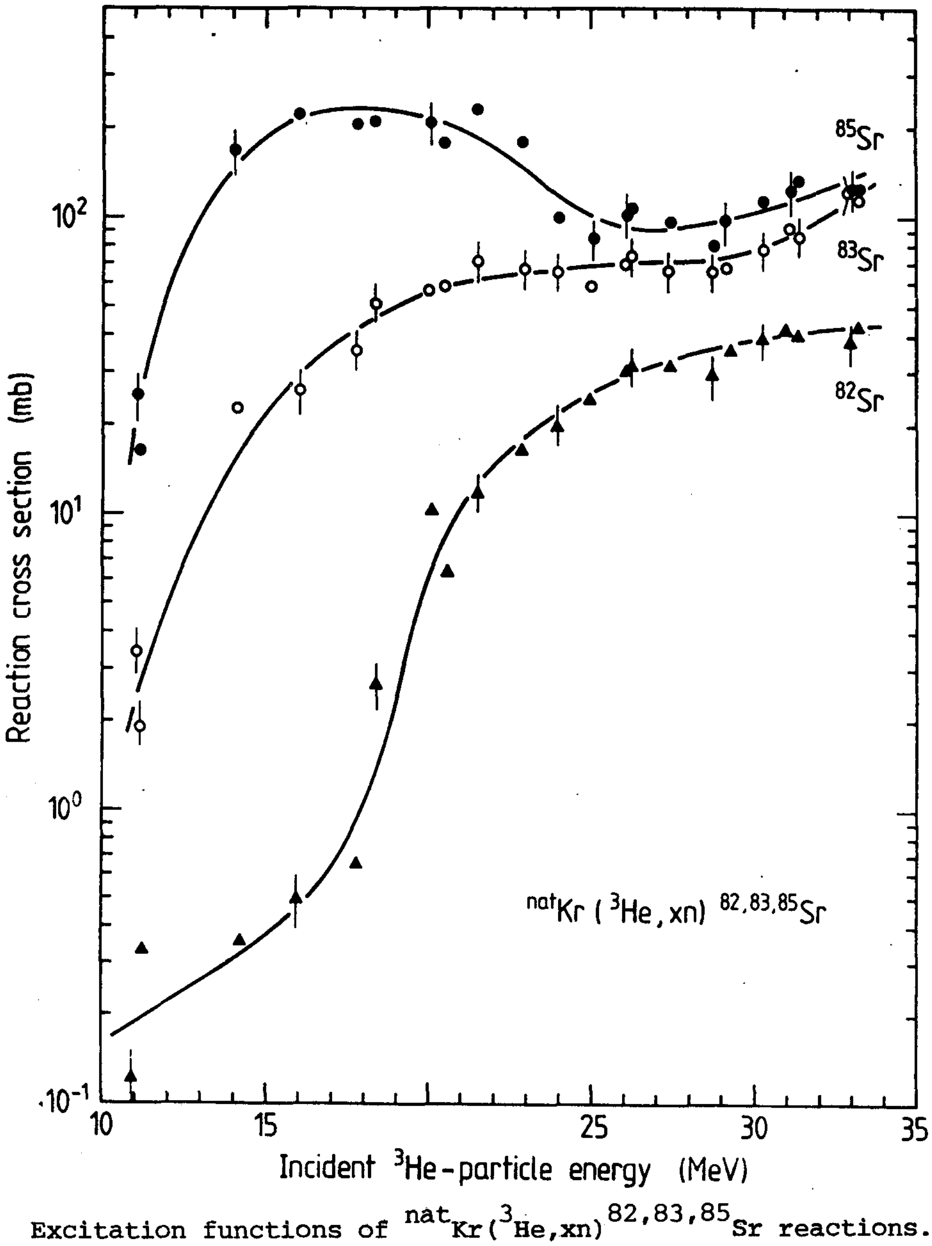

Fig. 3 Excitation functions of $^{nat}Kr(^{3}He,xn)^{82,83,85}Sr$ reactions.

References

[1] S.M. Qaim, R. Wölfle, H. Liskien, Excitation function of $^{93}Nb(n,{}^{3}He)^{91}Y$ reaction near its threshold: Comparison of ^{3}He and ^{3}H emission probabilities, Phys. Rev. C34 (1986) 489

[2] S.M. Qaim, R. Wölfle, $^{7}Li(n,n't)^{4}He$ reaction cross section via tritium counting, Nucl. Sci. Eng., in press

[3] A. Suhaimi, R. Wölfle, S.M. Qaim, G. Stöcklin, Measurement of $^{10}B(n,t)2\alpha$ reaction cross section in the energy range of 2.5 to 10.6 MeV: Diffusion of tritium in boron carbide, Radiochimica Acta, 40 (1986) 113

[4] H. Liskien, R. Widera, R. Wölfle, S.M. Qaim, Experimentally determined excitation function for the $^{9}Be(n,t)$ reaction, Nucl. Sci. Eng., submitted

[5] S.M. Qaim, A study of $(n,n\alpha)$ reaction cross sections at 14.7 MeV, Nucl. Phys. A458 (1986) 237

[6] S.M. Qaim, G. Blessing, H. Ollig, Excitation functions of $^{75}As(\alpha,n)^{78}Br$ and $^{75}As(\alpha,2n)^{77m,g}Br$ reactions from threshold to 28 MeV, Radiochimica Acta 39 (1986) 57

INSTITUT FÜR REAKTORENTWICKLUNG
KERNFORSCHUNGSANLAGE JÜLICH

1. (p,n) Cross Section Time of Flight Measurements

W. Amian, N. Paul, M.M. Meier[1], G.J. Russell[1], H. Robinson[1], R. Whitaker[1], G.L. Morgan[1], D. Holtkamp[1],

Neutron yields from proton bombardment of C, Al, Ni, W, Pb and depleted U have been obtained at bombarding energies of 800 and 318 MeV. Additionally, at 318 MeV, data were obtained for Be and Ta. The data were obtained at angles/flight-paths of 7deg/30 m, 15deg/30m, and 30deg/40m and were collected in two parameter histrograms of time-of-flight and pulse-height. Pulse-height information was obtained in order to facilitate the analysis by providing the possibility for post-experiment selection of bias and to permit comparison of calculated and experimental pulse height spectra in the calculation of detector efficiency. The experiment was designed to provide energy resolution better than 1% and statistical accuracy of 5% or better for any 1% energy bin. The data have been reduced to absolute double-differential cross sections.

The overall accuracy of the measurements is about 20-40% limited by the accuracy of the reference detector efficiency determination [1], the counting statistics, the attenuation uncertainties and the absolute accuracy of the proton monitor. Over the studied angular range, 7.5 to 30 degrees, the HETC code adequately describes the 800 MeV data but underestimates the data at 318 MeV by as much as a factor of 3. One set of double differential cross sections is shown in Fig. 1. Error bars on the experimental data points include the counting statistics and attenuation uncertainties, but do not include the uncertainties in the absolute value of shape of the efficiency or uncertainties due to charge and target thickness normalization. The calculations were done using the Los Alamos HETC/MCNP/HTAPE [2] code package.

---

[1]Los Alamos National Laboratory, USA

References

[1] S.D. Howe et al., Nucl. Instr. & Methods 193 (1982) 549

[2] R.E. Prael, User's Guide to the HETC Code System
Los Alamos National Laboratory, Internal Report, April 1985

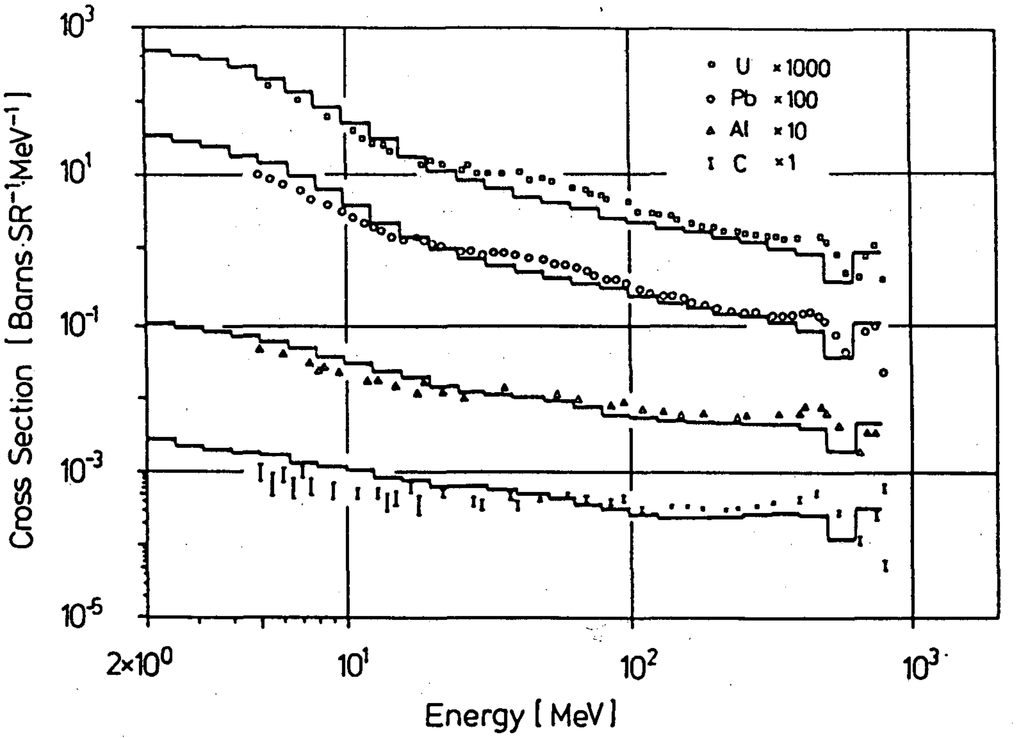

Fig. 1: Double differential cross section for proton induced neutron production at 800 MeV

2. A Medium Energy Neutron Deep Penetration Experiment - Experimental and Theoretical Analysis -

W. Amian, P. Cloth, V. Drüke, D. Filges, N. Paul, H. Schaal

We report on a deep penetration experiment conducted at the Los Alamos WNR facility's Spallation Neutron Target [1]. The experiments are compared with calculations to help validating those features of the present HETC/KFA-1 [2], and ANISN [3] codes installed at KFA-IRE which are applied to deep penetration problems for high-energy neutrons above 15 MeV (details see Ref. [4]).

For such problems the most reasonable technique to detect neutrons is by counting decaying residual nuclei of high energy interactions with suitable target materials. Especially for accelerator environments, spallation reactions on copper have been proposed by Routti [5] as a means to extend the known threshold-foil technique to higher hadron energies. The yield cross sections for many spallation products have a threshold type energy dependence with threshold energies of tens or hundreds of MeV. The advantage of these spallation detectors is that several gamma-active products with different threshold energies can be obtained from only one measurement.

The problem with these reactions, however, is that the spallation yield cross sections are basically not known above 20 MeV. While the experiments can reveal clearly the exponential decrease of reaction rates with shielding thickness without any prior knowledge of cross sections, the quantitative comparison between experiment and calculation suffers from the lack of reliable cross section data for these spallation yield cross sections. This deficiency was demonstrated by a comparison of experimental and theoretically determined production cross sections for some isotopes from natural copper.

References

[1] R. Woods
Proceedings of the 5th Meeting of International Collaboration on Advanced Neutron Sources (ICANS-V) Jülich, June 22-26, 1981, Jül-Conf-45, October 1981

[2] P. Cloth, D. Filges, G. Sterzenbach, T.W. Armstrong, B.L. Colborn
The KFA-Version of the High-Energy Transport Code HETC and the generalized Evaluation Code SIMPEL
Report Jül-Spez-196, March 1983

[3] W.W. Engle
Report ORNL-1693, 1973

[4] W. Amian, P. Cloth, V. Drüke, D. Filges, N. Paul, H. Schaal
A Medium Energy Neutron Deep Penetration Experiment - Experimental and Theoretical Analysis -
Jül-Report Jül-2101, November 1986

[5] J.T. Routti, J. Tapio
High-Energy Neutron Spectroscopy with Activation Detectors
Report UCRL-18514, 1969

GKSS-FORSCHUNGSZENTRUM GEESTHACHT GMBH
INSTITUT FÜR PHYSIK

14 Mev Neutron Activation Cross-Sections

R. Pepelnik, E. Bössow, Y. Tian

For activation analysis at the high intense neutron generator facility KORONA [1] some cross-sections have been remeasured. The cylindrical target structure of KORONA leads to a neutron energy distribution with a median at 14.7 MeV and a FWHM of 0.6 MeV [2]. For the neutron flux monitoring a long-counter is used. The long-counter is calibrated via the well-known reactions $^{27}Al(n,\alpha)$ and $^{93}Nb(n,2n)$.

Samples from material of high purity containing P, Cl and Zn were investigated. The reaction cross-sections determined are summarized in Table I.

Table I Activation Cross-Sections (mb) at 14.7 MeV

Reaction	This Work 14.7 ± 0.3 MeV	Literature [3] 14.5 MeV	 14.9 MeV
$^{31}P\ (n,\alpha)^{28}Al$	139. ± 5.	188. ± 15.	115. ± 12.
$^{37}Cl(n,p)^{37}S$	33.3 ± 1.2	33. ± 6.	41. ± 4.
$^{64}Zn(n,2n)^{63}Zn$	164. ± 6.	165. ± 13.	204. ± 16.

The neutron energy spectrum within the cylindrical target of KORONA also contains contributions from elastically and inelastically scattered neutrons. These contributions have been calculated [2,4] to 26 and 9 % of the total neutron flux, respectively. The scattered neutrons of lower energy and the low threshold of the P(n,α)-reaction might have increased the effective activation cross-section.

References

[1] H.-U. Fanger, R. Pepelnik, W. Michaelis, J. Radioanal. Chem. 61 (1981) 147.
[2] B.M. Bahal, H.-U. Fanger, Nucl. Instr. and Meth. 211 (1983) 469.
[3] M. Bormann, H. Neuert, W. Scobel, in Handbook on Nuclear Activation Cross-Sections, Techn. Rep. Ser. N. 156, IAEA 1974, Vienna.
[4] A. Pavlik, G. Winkler, Inst. für Radiumforschung und Kernphysik der Universität Wien, to be published.

I. INSTITUT FÜR EXPERIMENTALPHYSIK
UNIVERSITÄT HAMBURG

Shell Effects in Pb(p,xn) Preequilibrium Neutron Emission

K. Harder, A. Kaminsky, E. Mordhorst, W. Scobel, M. Trabandt

The neutron time-of-flight spectrometer [1] at the Hamburg Isochronous Cyclotron allows to measure continuous spectra for $3° \leq \theta \leq 177°$ down to the 10-100 μb/sr·MeV level. We have studied with 25.5 MeV projectiles the influence of shell effects in the typical preequilibrium (PE) region of the neutron energy spectra from the reactions ^{204,206,207,208}Pb(p,xn) and the PE emission into the backward hemisphere. Measurements in the forward hemisphere $\theta_{lab} \leq 60°$ have been performed with an extended (20 m instead of 7.5 m) time-of-flight path to improve the resolution. The results can be summarized as follows:

We have found evidence (cf. Fig. 2) that strong deviations of single particle state densities from those of a Fermi gas influence the neutron PE emission in (p,n) reactions from nuclei as $^{204-208}_{\ \ \ \ \ \ \ 93}$Bi. The general spectral shape of the PE continuum may be accounted for by lowering [2] the s.p. level density $\underline{g}$ to values known [3] from compound nucleus reactions at low excitation (Fig. 1). The structures at the high energy end could be related to the nearby double shell closure; they correspond to the broader structures observed for sequences of nuclei crossing the $f_{7/2}$ or $g_{9/2}$ shell closure [4]. A more quantitative understanding will probably require the consideration of angular momentum coupling.

The data obtained for $^{204-208}$Pb(p,xn) are available upon request in tabular form.

References

[1] Y. Holler, A. Kaminsky, B. Scharlemann, H. Krause, R. Langkau, W. Peters, G. Poppe, N. Schirm, W. Scobel and R. Wien
Nucl. Instr. Meth. 235(1985)123

[2] K. Harder, A. Kaminsky, E. Mordhorst, W. Scobel and M. Trabandt, to be published (1987)

[3] L.F. Hansen, M. Blann, R.J. Howerton, T.T. Komoto and B.A. Pohl, Nucl. Sci. Eng. 92(1986)382

[4] M. Blann, S.M. Grimes, L.F. Hansen, T.T. Komoto, B.A. Pohl, W. Scobel, M. Trabandt and C. Wong, Phys. Rev. C32(1985)411

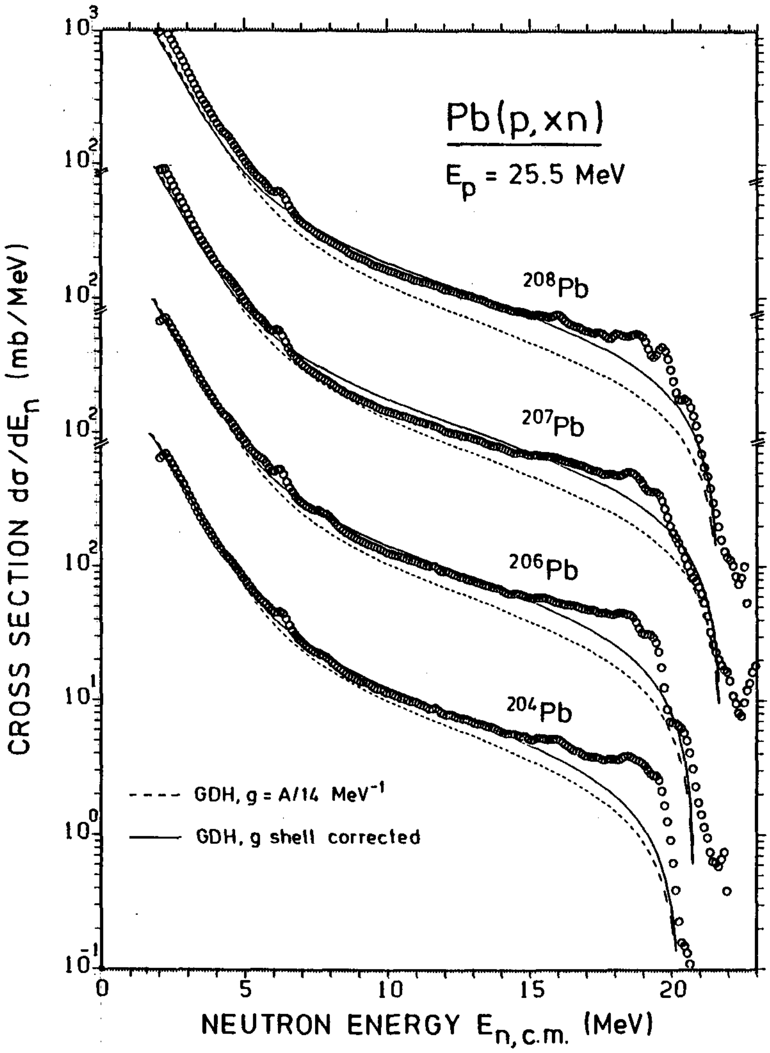

Fig. 1: Experimental (open circles) angle integrated neutron energy spectra compared to GDH model calculations with standard (g = A/14 MeV^{-1}, dashed line) and shell corrected (g = A/26 MeV^{-1} (^{208}Bi),...,A/20 MeV^{-1} (^{204}Bi), solid lines) single particle level density.

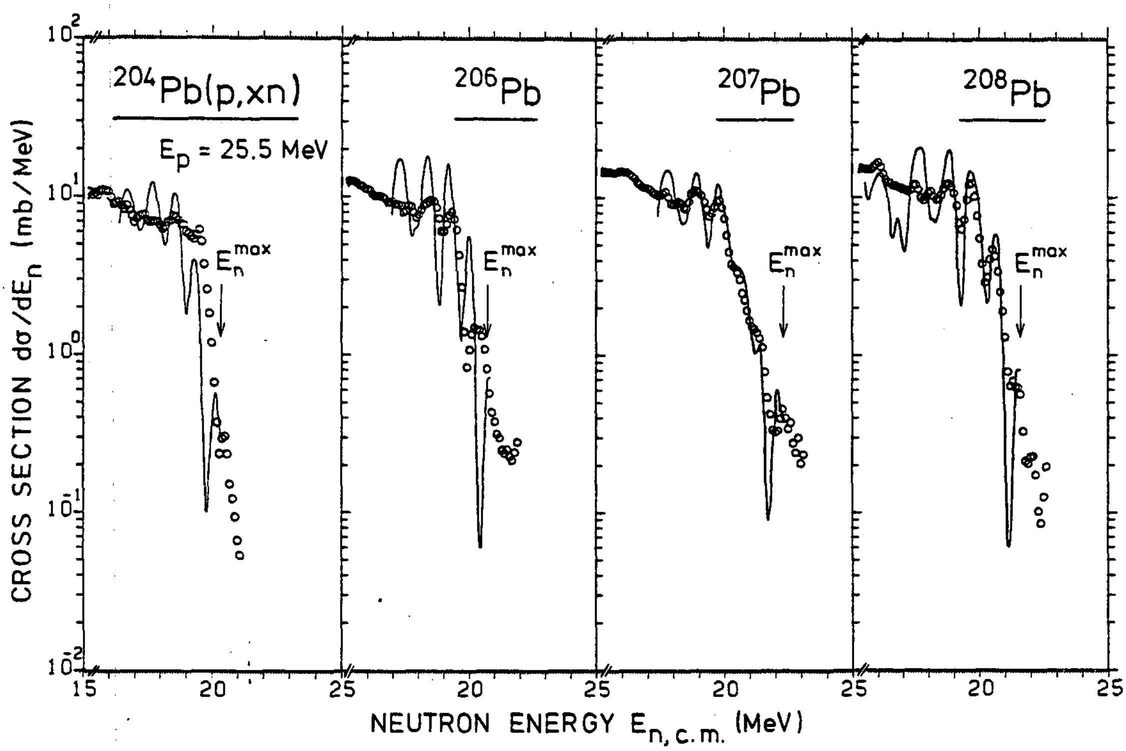

Fig. 2: High energy part of the Pb(p,xn) spectra in the forward cone $\theta_{lab} \leq 60°$. The solid line is the microscopically calculated 1p1n^{-1} state density.

INSTITUT FÜR BIOCHEMIE, ABTEILUNG NUKLEARCHEMIE
UNIVERSITÄT ZU KÖLN

1. Thin Target and Thick Target Data Relevant for the Interpretation of Cosmogenic Nuclides in Meteorites

P. Dragovitsch, F. Peiffer, S. Theis, R. Michel*

1.1 Experimental and Theoretical Production Rates of Spallogenic Nuclides in Artificial Meteorites

Approximately 450 depth profiles of stable and radioactive nuclides have been measured for a large variety of target materials in thick spherical stony targets with radii of 5, 15 and 25 cm isotropically irradiated with 600 MeV protons at the CERN synchrocyclotron. These irradiation experiments (CERN SC96, Cologne Collaboration) were intended to simulate the irradiation of meteoroids by galactic cosmic ray protons. (Since the shape of a meteorite found on the earth's surface usually differs strongly from that before atmospheric transit, the term meteoroid is used for meteoritic objects in space.) While gamma-spectrometric measurements have been finished, further investigations by conventional mass spectrometry (Xe, Ar) and by accellerator mass spectrometry (^{10}Be, ^{14}C, ^{26}Al, ^{41}Ca, etc.) are still under way. In order to combine this experimental approach with a theoretical one the intra- and internuclear particle cascades caused by the irradiation with 600 MeV protons were calculated using Monte Carlo techniques via the high energy transport code HET/KFA 1 [1]. Together with transport calculations for low energy neutrons by the MORSE-CG code [2] thus the depth dependent spectra of primary and secondary protons and of secondary neutrons were derived. On the basis of these spectra and of a

* Zentraleinrichtung für Strahlenschutz, Universität Hannover. This report describes a joint project of the Abteilung Nuklearchemie and the Zentraleinrichtung für Strahlenschutz.

set of evaluated experimental excitation functions for p-induced reactions and of theoretical ones for n-induced reactions calculated by the code ALICE LIVERMOORE 82 [3] theoretical depth profiles for the production of stable and radioactive nuclides in the three thick targets were calculated. In order to handle the enormous amount of experimental and theoretical results and to provide a detailed data base for further discussions a comprehensive report was prepared containing all those target/product combinations for which both experimental and theoretical data are available [4]. It covers about 300 depth profiles for 101 reactions. The remaining reactions are not covered because of an absolute lack of thin target excitation functions in these cases. The agreement between experimental and calculated depth profiles is generally excellent, though there are differences in the quality of agreement. For a large number of reactions it is better than 5 to 10% (e.g. fig. 1 A). Most of the depth profiles agree with the calculations at least within 20% (fig. 1 B). Most still existing discrepancies between theory and experiment can be attributed to an insufficient knowledge of the underlying excitation functions. Here further work on thin target excitation functions is needed. Only some exceptional cases e.g. ^{7}Be from Fe (fig. 1 C) exhibit differences which not simply can be explained by an insufficient knowledge of exitation functions. Such discrepancies are seen for those high energy products for which the production as residual nuclide is competing with the possible production by cluster emission during an early phase of the reaction. The experimental observation is that for these nuclides the secondary production nearly exactly counterweighs the decrease of primary production throughout the entire sphere, thereby resulting in completely flat depth profiles which are not reproduced by theory. In spite of these problems the experimental and theoretical data now allow for a detailed discussion of the different production modes of cosmogenic nuclides clearly distinguishing reactions of the various contributing particles. They provide a basis for an advanced modelling of the production of cosmogenic nuclides in meteoroids by galactic cosmic ray protons. Moreover, they permit a validation of the high energy transport calculations.

1.2 Thin Target Cross Sections for p-Induced Reactions at 600 MeV

Considering the fact that for a considerable number of nuclear reactions only few and often insufficient thin target cross section data are availab

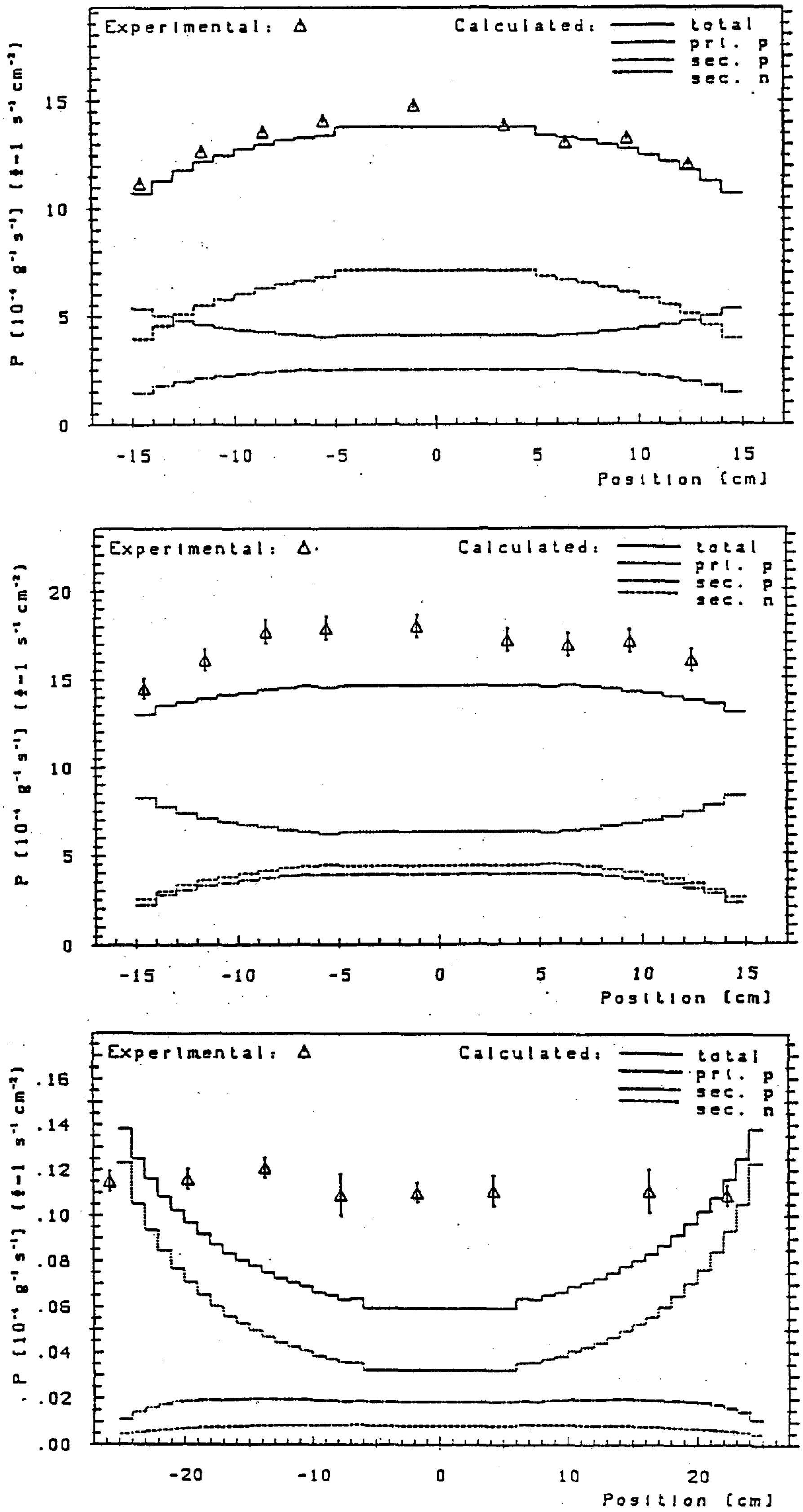

Fig. 1: Experimental and theoretical production depth profiles of ^{21}Ne from Mg (A) and ^{22}Ne from Mg (B) in an artificial meteoroid with 15 cm radius and of ^{7}Be from Fe (C) in one with 25 cm radius.

le a systematic study on thin target cross sections for the production of stable and radioactive nuclides has been started. Here we report on the results of cross section measurements of gamma-emitting radionuclides produced by 600 MeV protons from the elements O, Mg, Al, Si, Ti, Cr, Fe, Ni and Cu. The determination of cross sections for rare gas isotope production and for longlived radionuclides which have to be measured by conventional and accellerator mass spectroscopy are still underway. A comparison of the new experimental data with those reported earlier partially showed severe discrepancies and the need to revise a large number of older data (see [5] for a detailed discussion). For a first theoretical interpretation the experimental data were compared with calculations based on the work of Rudstam [6] and of Silberberg und Tsao [7]. The comparison of experimental and theoretical data (table 1) demonstrates that the semi-empirical formulas for the calculation of spallation cross sections are only suitable as rough estimates and by no means allow for an accurate description of these high energy reactions. The observed discrepancies between theory and experiment call for the more detailed modelling of nuclear reactions in the transition region from preequilibrium to spallation reactions. Here it is of particular interest that a recent versions of the hybrid model of preequilibrium reactions now allows for a priori calculations of nuclear reaction data up to proton energies of 300 MeV [8]. Further work is in progress to extent these calculations to even higher energies thus hopefully allowing for more detailed insight into nuclear reaction mechanisms at these energies. The experiments will be continued laying emphasis on those (mono-isotopic) elements which allow for an easier discussion of the systematics of spallation nuclear reactions in particular of the transition from preequilibrium to spallation.

<u>References</u>

[1] P. Cloth, D. Filges, G. Sterzenbach, T.W. Armstrong, B.L. Colburn, Jül-Spez-196 (1983).

[2] M.B. Emmett, ORNL - 4972 (1975).

[3] M. Blann, J. Bisplinghoff, UCID - 19614 (1982).

[4] Cologne Collaboration, Jül-Spez (1987), in press.

[5] P. Dragovitsch, Thesis, Universität zu Köln (1987).

[6] G. Rudstam, Z. Naturf. 21a (1966) 1027.

[7] R. Silberberg, C.H. Tsao, Astrophys. J. Suppl. 25 (1973) 315.

[8] M. Blann, priv. comm. (1987).

Table 1: Experimental thin target cross sections for p-induced reactions at 600 MeV compared with semiempirical calculations acc. to refs. [6,7]. The abbreviations CDMDG and CDMD refer to two different versions of Rudstam's formula [6]. * monitor cross section.

Reaction	Cross Sections /mb/			
	Experimental	Calculated		
	this work	CDMDG	CDMD	Ref. 7
O(p,5pxn)^{7}Be	11.3 ± 0.5	1.69	1.55	7.91
Mg(p,9pxn)^{7}Be	6.43 ± 0.28	0.514	0.522	3.79
Mg(p,2pxn)^{22}Na	31.5 ± 1.3	20.4	18.3	20.3
Mg(p,2pxn)^{24}Na	7.94 ± 0.38	30.9	29.2	9.66
Al(p,10p11n)^{7}Be	4.88 ± 0.10	0.35	0.367	2.83
Al(p,3p3n)^{22}Na	16.0 *)	13.9	12.9	14.1
Al(p,3pn)^{24}Na	11.3 ± 0.3	21.1	20.6	9.53
Si(p,11pxn)^{7}Be	5.39 ± 0.22	0.299	0.318	2.84
Si(p,4pxn)^{22}Na	19.6 ± 0.6	11.9	11.2	14.8
Si(p,4pxn)^{24}Na	5.15 ± 0.19	18.0	17.8	0.578
Ti(p,19pxn)^{7}Be	1.95 ± 0.09	0.0176	0.0174	1.72
Ti(p,12pxn)^{22}Na	0.90 ± 0.04	0.696	0.837	0.989
Ti(p,12pxn)^{24}Na	1.37 ± 0.09	1.06	1.33	1.42
Ti(p,4pxn)^{42}K	9.01 ± 0.48	12.4	10.5	6.37
Ti(p,4pxn)^{43}K	3.68 ± 0.24	3.80	2.90	2.10
Ti(p,3pxn)^{47}Ca	0.26 ± 0.01	0.190	0.240	0.163
Ti(p,2pxn)^{44m}Sc	7.21 ± 0.29	-	-	-
Ti(p,2pxn)^{46}Sc	32.0 ± 1.2	37.0	33.7	19.4
Ti(p,2pxn)^{47}Sc	28.4 ± 1.1	15.3	10.9	7.88
Ti(p,2pxn)^{48}Sc	2.97 ± 0.14	3.77	2.76	1.73
Ti(p,xn)^{48}V	1.9 ± 0.08	46.9	44.5	39.7
Cr(p,14pxn)^{22}Na	2.48 ± 0.20	0.382	0.483	0.607
Cr(p,6pxn)^{43}K	6.18 ± 0.59	2.09	1.67	0.982
Cr(p,5pxn)^{47}Ca	0.22 ± 0.03	0.104	0.139	0.0693
Cr(p,4pxn)^{44m}Sc	31.4 ± 1.8	-	-	-
Cr(p,4pxn)^{46}Sc	48.1 ± 2.8	19.6	18.7	9.77
Cr(p,4pxn)^{47}Sc	20.0 ± 1.1	8.41	6.32	3.73
Cr(p,4pxn)^{48}Sc	3.60 ± 0.22	2.07	1.59	0.773

Table 1: continued

Reaction	Cross Sections /mb/				
	Experimental		Calculated		
	this work		CDMDG	CDMD	Ref. 7
$Cr(p,2pxn)^{48}V$	77.4	± 4.3	25.7	25.7	26.0
$Cr(p,pxn)^{48}Cr$	2.11	± 0.13	1.13	1.11	1.91
$Cr(p,pxn)^{51}Cr$	180.1	± 9.9	61.6	76.6	71.7
$Cr(p,xn)^{52}Mn$	1.38	± 0.12	33.1	28.8	30.4
$Fe(p,23pxn)^{7}Be$	2.01	± 0.09	0.0055	0.00825	1.79
$Fe(p,16pxn)^{22}Na$	0.40	± 0.03	0.218	0.290	0.396
$Fe(p,8pxn)^{43}K$	0.95	± 0.05	1.19	1.00	0.437
$Fe(p,6pxn)^{44m}Sc$	8.4	± 0.3	-	-	-
$Fe(p,6pxn)^{46}Sc$	9.44	± 0.37	11.2	11.2	4.73
$Fe(p,6pxn)^{47}Sc$	2.89	± 0.11	4.80	3.79	1.67
$Fe(p,4pxn)^{48}V$	22.7	± 0.8	14.7	15.4	18.7
$Fe(p,3pxn)^{48}Cr$	0.615	± 0.12	0.647	0.666	1.57
$Fe(p,3pxn)^{51}Cr$	46.3	± 1.7	35.2	46.0	49.0
$Fe(p,2pxn)^{52}Mn$	11.5	± 0.6	18.9	17.2	22.8
$Fe(p,2pxn)^{54}Mn$	39.8	± 1.5	60.0	77.5	52.9
$Fe(p,xn)^{56}Co$	1.36	± 0.06	21.5	17.9	25.8
$Fe(p,xn)^{57}Co$	0.23	± 0.01	63.7	63.0	91.5
$Fe(p,xn)^{58}Co$	0.036	± 0.007	-	-	-
$Ni(p,25pxn)^{7}Be$	2.63	± 0.12	0.0037	0.0057	1.98
$Ni(p,18pxn)^{22}Na$	0.39	± 0.03	0.146	0.200	0.393
$Ni(p,8pxn)^{46}Sc$	5.03	± 0.19	7.47	7.74	1.98
$Ni(p,6pxn)^{48}V$	22.7	± 0.9	9.81	10.6	17.9
$Ni(p,5pxn)^{48}Cr$	1.86	± 0.10	0.433	0.46	2.24
$Ni(p,5pxn)^{51}Cr$	42.8	± 1.6	23.5	31.7	29.4
$Ni(p,4pxn)^{52}Mn$	15.8	± 0.6	12.6	11.9	24.7
$Ni(p,4pxn)^{54}Mn$	16.4	± 0.7	40.1	53.6	24.2
$Ni(p,3pxn)^{59}Fe$	0.30	± 0.02	10.1	6.37	1.47
$Ni(p,2pxn)^{56}Co$	38.4	± 14.3	12.3	31.3	
$Ni(p,2pxn)^{57}Co$	75.6	± 2.8	42.6	43.6	85.8
$Ni(p,2pxn)^{58}Co$	23.4	± 0.9	74.9	101.0	62.6
$Ni(p,2pxn)^{60}Co$	2.31	± 0.22	52.2	38.0	10.4

Table 1: continued

Reaction	Cross Sections /mb/			
	Experimental	Calculated		
	this work	CDMDG	CDMD	Ref. 7
Ni(p,pxn)^{56}Ni	2.25 ± 0.19	0.261	0.374	2.54
Ni(p,pxn)^{57}Ni	23.7 ± 0.9	2.57	2.43	9.50
Cu(p,26pxn)^{7}Be	1.61 ± 0.08	0.0018	0.003	0.619
Cu(p,19pxn)^{22}Na	0.136 ± 0.017	0.0716	0.104	0.297
Cu(p,11pxn)^{43}K	0.507 ± 0.027	0.390	0.361	0.287
Cu(p,9pxn)^{44m}Sc	3.85 ± 0.20	-	-	-
Cu(p,9pxn)^{46}Sc	5.5 ± 0.21	3.66	4.04	2.89
Cu(p,9pxn)^{47}Sc	2.33 ± 0.09	1.57	1.36	1.09
Cu(p,7pxn)^{48}V	11.1 ± 0.4	4.81	5.55	5.70
Cu(p,6pxn)^{51}Cr	27.7 ± 1.0	11.5	16.5	16.2
Cu(p,5pxn)^{52}Mn	9.35 ± 0.35	6.19	6.21	6.78
Cu(p,5pxn)^{54}Mn	23.1 ± 0.9	19.7	27.9	20.9
Cu(p,4pxn)^{59}Fe	1.7 ± 0.2	4.97	3.32	2.24
Cu(p,3pxn)^{56}Co	10.3 ± 0.4	7.03	6.43	7.77
Cu(p,3pxn)^{57}Co	27.7 ± 1.0	20.9	22.7	29.2
Cu(p,3pxn)^{58}Co	34.4 ± 1.4	36.7	52.5	45.3
Cu(p,3pxn)^{60}Co	11.9 ± 0.5	25.6	19.8	13.3
Cu(p,2pxn)^{57}Ni	1.0 ± 0.04	1.26	1.27	1.80

INSTITUT FÜR KERNCHEMIE
UNIVERSITÄT MAINZ

Decay Properties of $^{96m,g}Y$

H.O. Denschlag, H. Faust*, U. Güttler, St. Hörner und P. Stumpf.

Fission products of the decay chain with mass number A=96 produced in $^{235}U(n_{th},f)$ were separated in the mass separator LOHENGRIN (Grenoble, France). The beam of fragments left the separator trough a thin mylar window and was intercepted in a He-jet chamber. The fission products adsorbed on clusters of KCl were carried to a glass fiber filter and deposited there. A HP Ge-detector mounted directly opposite the filter allowed to measure ß-rays and the conversion electrons emitted in the decay of 6 s isomer of ^{96}Y [0^-] and a Ge(Li)-gamma-ray detector mounted at 90 degrees allowed to measure the gamma-rays emitted in the decay of the 10 s isomer of ^{96}Y ["High spin"]. The two detectors were carefully calibrated relative to each other using commercial gamma-ray standards placed in the filter position and using a ^{207}Bi-source for gamma rays and conversion electrons. In order to correct for the energy loss of conversion electrons in the filter the measurement of the ^{207}Bi source was measured directly in front of the detector and behind the filter containing the clusters and the ^{96}Y activity. The energy loss of the conversion electrons in the filter was found to amount to 5 keV nearly independent of their energy.

The following results were obtained. The energy of the conversion electrons emitted in the decay of 6 s ^{96}Y amounts to 1566$\pm$2 kev. This brings the first excited level of ^{96}Zr to 1584 keV rather than the value of 1594 keV given in the literature [1].

----

*Institut Laue-Langevin, Grenoble (France)

In addition, the feeding of this level as obtained by a comparison of conversion events with the total ß-events was found 0.5 (+0.5/-0.3) %, i.e. considerably smaller than the 25 % indicated in Ref. 1. The value given above was found for different kinetic energies and ionic charge states (q) of the fragments as separated in LOHENGRIN. The error margins indicated cover any uncertainties due to possible contaminations by mass chains of similar A/q. The present findings are confirmed by van Klinken et al. [2].

References

[1] C.M. Lederer, V.S. Shirley Eds., Table of Isotopes, J. Wiley, New York (1978).

[2] J. van Klinken, J.F.W. Jansen, W.Z. Venema, and B. Pfeiffer, E0 Transitions after (α,xn) and (α,f) Reactions in Actinide Targets, Paper presented at International Conference on Nuclear Structure, Reactions, and Symmetries, Dubrovnik, June 1986.

INSTITUT FÜR KERNCHEMIE
PHILIPPS-UNIVERSITÄT MARBURG

1. Gamma-Ray Catalog
W. Westmeier

Quantitative information on gamma rays from the decay of radioactive nuclides is required in many areas of nuclear science as well as related fields. We have therefore produced a compilation of decay properties of all known radionuclides, with the main emphasis on energies and absolute intensities of the gamma rays. A first printed version of this catalog was issued in 1979, and a second edition, including references through June 1982, was completed in 1983. The second version contains information on 2526 nuclides and isomers with a total of more than 47.000 gamma rays and X-rays, the information on X-rays accompanying radioactive decay being a newly introduced feature. The catalog is presented in two parts: In Part I gamma rays are listed in order of increasing energy for the purpose of identification of unknown gamma lines. In Part II complete data sets for each nuclide are listed in order of mass number A and nuclear charge Z of the nuclides. This part also contains additional information, references, and comments in any case of discrepancies.
The second version of the catalog was published in "Atomic Data and Nuclear Data Tables", Volume 29, Nos. 1,2 (1983).
At present, a third and completely updated version of the catalog is in preparation where the literature cutoff date is estimated to be about 1987.

2. Alpha-Particle Catalog
W. Westmeier, A. Merklin

A table of alpha-decay properties of all known alpha-emitting nuclides, which includes data on alpha energies, intensities, and the abundances of the alpha branch, has been compiled. The table is laid out in a manner similar to the Gamma-Ray Catalog and it has been published in "Physik Daten/ Physics Data", Nr. 29-1, Fachinformationszentrum Energie Physik Mathematik GmbH, Karlsruhe, 1985, ISSN 0344-8401.

Both tables are compiled and updated under the auspicies of the Fachinformationszentrum Energie Physik Mathematik GmbH (FIZ) in Karlsruhe.

REAKTORSTATION GARCHING, FACHBEREICH PHYSIK
TECHNISCHE UNIVERSITÄT MÜNCHEN

A) Coherent Neutron Scattering Lengths and Total Cross Sections

1. Interaction of Slow Neutrons with the Isotopes of Molybdenum

L.Koester, K.Knopf, W.Waschkowski

Coherent neutron scattering lengths and total cross sections were measured on samples of ordinary Mo and isotopically enriched samples. From the experiments with neutrons of 0.57 meV and 1.26 eV the following values have been obtained:
- the coherent scattering lengths (in fm) of the bound atoms of Mo (6.715±0.020) and for the isotopes with the mass numbers 92 (6.93±0.08), 94 (6.82±0.07), 95 (6.93±0.06), 96 (6.22±0.06), 97 (7.26±0.08), 98 (6.60±0.07) and 100 (6.75±0.07);
- the incoherent scattering cross section at zero-energy for ordinary Mo: σ_i=0.02±0.02 barn;
- the absorption cross sections (in barn) for Mo (2.48±0.04) and for the isotopes with the mass numbers 95 (13.4±0.3), 97 (2,5±0.2) and 100 (0.4±0.2). The relation of the present results to the resonance parameters of the neutron - Mo interaction has been discussed.

Z. Phys. A - Atomic Nuclei 326, 227-231 (1987)

2. Neutron Interactions with Germanium Isotopes and Amorphous and Crystalline GeO_2

L.Koester, K.Knopf, W.Waschkowski

Coherent neutron scattering lengths and total cross sections have been measured on elemental and oxide samples of ordinary Ge and of isotopically enriched substances. From the experimental results the following values were obtained:
- the coherent scattering lengths (in fm) of the bound atoms Ge (8.185±0.020); ^{70}Ge (10.0±0.1); ^{72}Ge(8.51±0.10); ^{73}Ge(5.02±0.04); ^{74}Ge(7.58±0.10) and ^{76}Ge(8.2±1.5);
- the absorption cross sections at 0.0253 eV (in barn) for Ge(2.20±0.04): ^{70}Ge(2.9±0.2); ^{72}Ge(0.8±0.2); ^{73}Ge(14.4±0.4) and ^{74}Ge(0.4±0.2);

- the free cross sections for epithermal neutrons and the zero energy scattering cross sections.

On the basis of this data, the isotopic- and spin-incoherent cross sections have been determined and discussed.
Transmission measurements at 0.57 meV on amorphous and crystalline GeO_2 yielded for the amorphous sample an inelastic cross section eight times larger than for the crystalline samples. This effect corresponds to a clearly higher density of low energy states in the amorphous than in the crystalline substances.

Submitted to Z. Phys. A - Atomic Nuclei

B) Neutron Strength Function

1. Experimental Study on the 3P Size-Resonance in the p-Wave Neutron Strength Function

L. Koester, W.Waschkowski, J.Meier

Using a silicon filtered fission neutron beam of an energy width of 20 keV around 143 keV we measured the total cross sections for 37 nuclides and elements having mass numbers between 87 and 140 and determined the p-wave strength functions. The 3P-resonance at A = 98 shows no splitting into the $P_{3/2} - P_{1/2}$ doublet.
The narrow resonance peak and the following broad distribution of the p-strength function (A = 103 to 140) can approximately be reproduced by deformed optical model calculations. The spin-orbit term in the optical potential is consistent with the spin orbit force in the shell model. For nuclei around the closed (N = 50) neutron shell a shell effect in the p-wave stregth function is indicated.

Z. Phys. A - Atomic Nuclei 326, 185 - 190 (1987)

INSTITUT FÜR KERNENERGETIK UND ENERGIESYSTEME
UNIVERSITÄT STUTTGART

Investigation of the Intra- and Intermolecular Neutron Scattering Dynamics in Liquid Hydrogen and Deuterium for Calculating Neutron Cross-Sections*)

J. Keinert, M. Mattes, J. Sax

A model adequate for the liquid phase was derived to improve the neutron scattering dynamics reported by KOPPEL, YOUNG /1/. There the intramolecular spin dependence, the molecular rotations and vibrations are considered exactly. The translational modes represent the free molecule, which is a very poor assumption for the liquid in the energy range of cold neutrons. At IKE, we assumed for the translational modes a frequency distribution as in the solid phase and a hindered translation /2/. All motions are thought to be independent, so that the scattering cross-section data could be derived by calculating separate scattering laws. The final result we got by linking these by the convolution theoreme. The scattering laws are available in ENDF-5 format for the ortho- and para-modifications at different temperatures. Because of the violation of the principle of detailed balance (spin-rotational coupling connected with a change in moderator modification) the generated scattering laws $S(\alpha,\beta)$ must be extended to negative β. Therefore the scattering matrix generation code NJOY /3/ is modified at IKE to generate scattering matrices for 165 neutron energy groups up to 3 eV for transport calculations (cold neutron sources).
Especially for D_2, the intermolecular neutron scattering is important for cold neutron energies. First models to describe this scattering now are under investigation (e.g. hard-core model).
In the following figures some of our results for neutron cross-sections are represented.

References

/1/ Young, J.A.; Koppel, J.U.: Slow Neutron Scattering by Molecular Hydrogen and Deuterium. Phys. Rev. 135, A603 (1964)
/2/ Sax, J.: Berechnung von Wirkungsquerschnitten für die Streuung langsamer Neutronen an flüssigem Wasserstoff und Deuterium. Stuttgart: IKE, 1986 (IKE 6D-53)
/3/ Mac Farlane, R.E.; Muir, D.W.; Boicourt, R.M.: The NJOY Nuclear Data Processing System. Vol. II: The NJOY, RECONR, BROADR, HEATR, and THERMR Modules. LA-9303-M (ENDF-324) (1982)

*) gefördert vom BMFT, Projekt 'Erforschung kondensierter Materie und Atomphysik'

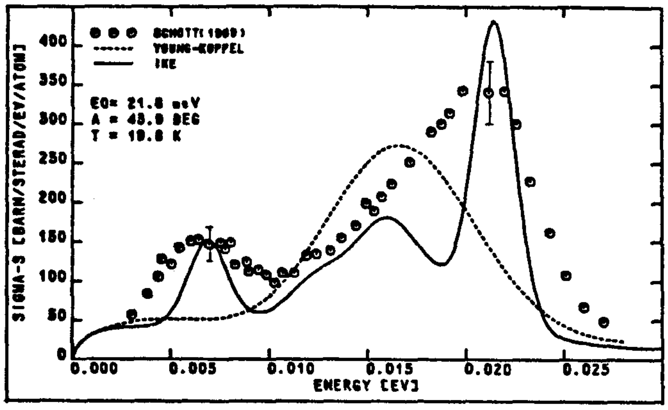

Fig. 1: Double-differential neutron scattering cross-sections for liquid hydrogen (para-H_2 = 52 %)

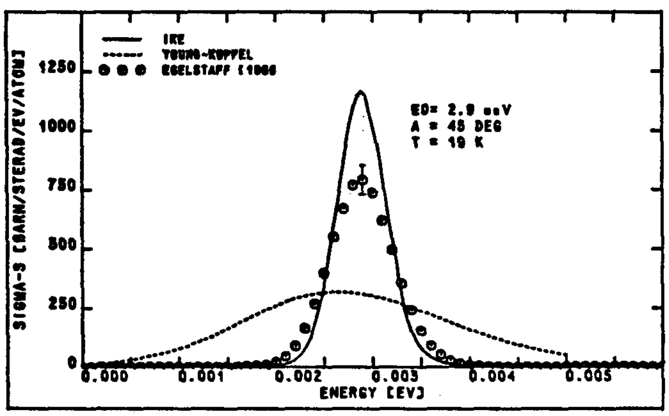

Fig. 2: Double-differential neutron scattering cross-sections for liquid D_2 (para-content 33.3 %)

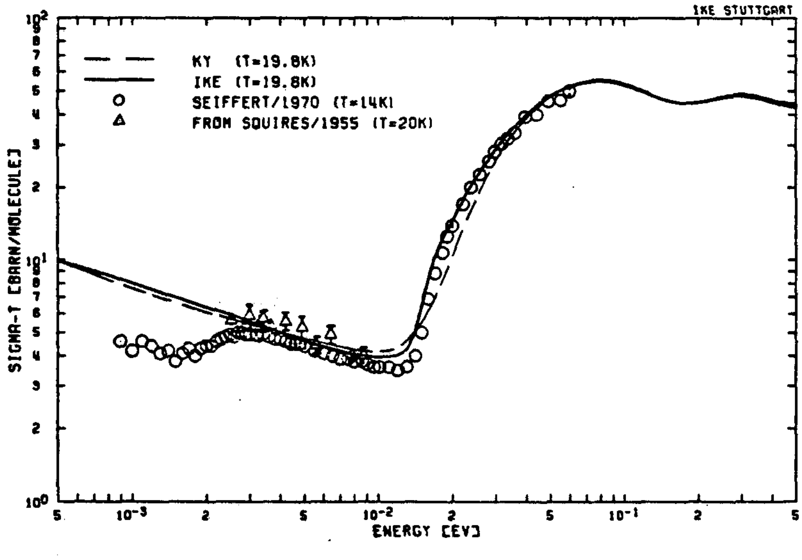

Fig. 3: Total neutron cross-sections for liquid para-hydrogen (H_2) at T = 14 K

INSTITUT FÜR STRAHLENPHYSIK
UNIVERSITÄT STUTTGART

1. Optical Model Analysis for ^{28}Si, ^{31}P, ^{32}S Using Polarized Neutron Scattering Data.

M. Koch, G. Bulski, W. Grum, K.-W. Hoffmann, G. Schreder, W. Weiß and J.W. Hammer

For the nuclei ^{28}Si, ^{31}P, ^{32}S scattering data were taken using the SCORPION [1] facility at E_n = 7.75 MeV. For the case of ^{28}Si a further investigation at E_n = 7.58 MeV was done. The scattering probes were made of material of high purity (better 99.9 %) and had a diameter of 40 mm and a height of 50 mm with a weight of 146.4 (Si), 101.4 (P) and 122.3 (S) grams. The polarized neutrons were produced using the $^{9}Be(\alpha,n)^{12}C$ - reaction and had an energy width of 140 keV (Si, S) or 240 keV (P). After unfolding the raw data with the FANTI code elastic and inelastic scattering could be separated within the resolution of the detectors (0.8 MeV). Corrections for finite geometry were obtained using a modified version of the code JANE.

The contribution of compound-elastic and -inelastic scattering was calculated within some restrictions using the CERBERO code [2] for the nuclei ^{28}Si and ^{32}S. All optical model calculations were performed with the new code ECIS 87 of J. Raynal [3], which allowed also in the case of ^{28}Si to calculate transmission coefficients for a deformed nucleus in a rotational model. Some level densities were further calculated according to the formalism of Gilbert and Cameron [4]. The transmission coefficients for the energy levels could be calculated from the spherical optical model, which leads however to some extent to an overestimation of the compound nucleus contributions. The Hauser Feshbach calculations were corrected in the manner of Moldauer [5], which takes into account the fluctuations in the level widths and the overlapping of levels. A few typical results from our work are shown in Figs. 1 and 2.

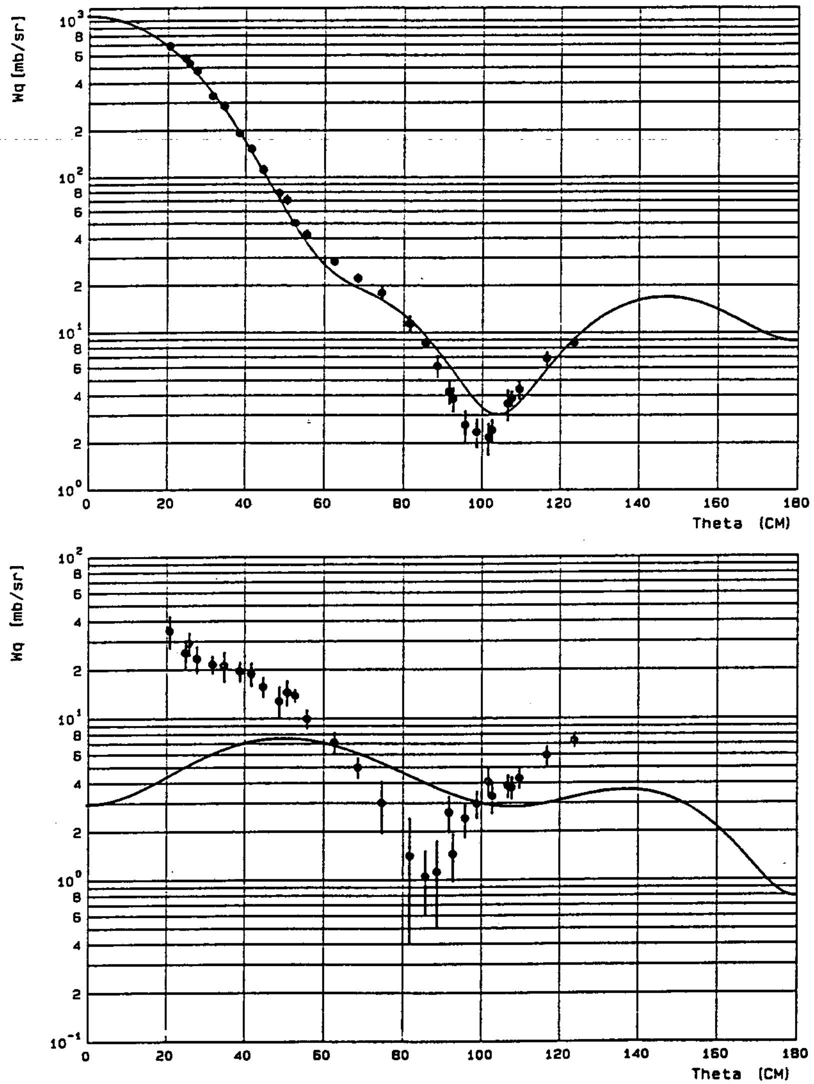

Figs. 1a/b Elastic and inelastic differential cross section of sulfur 32 for neutrons of E_n = 7.75 MeV. The lines indicate the results of a cc-analysis with the parameter set of Tab. 1.

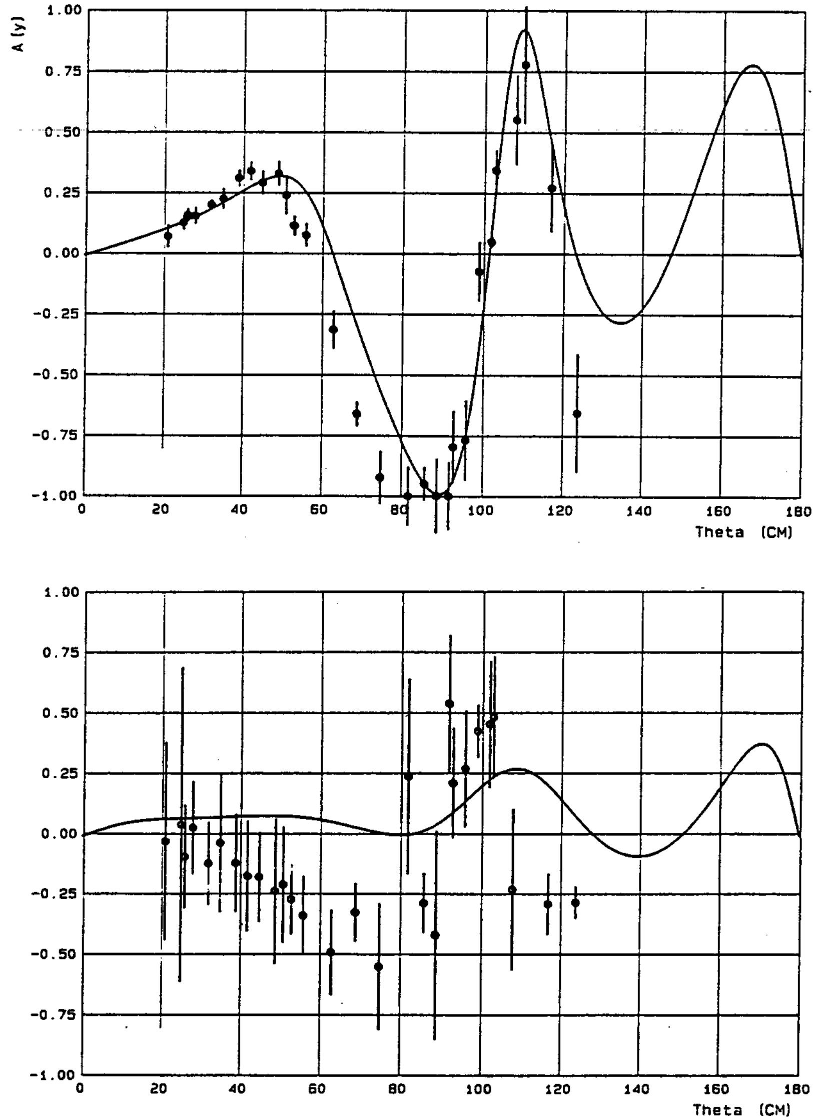

Figs. 2a/b Analyzing power for elastic and inelastic neutron-scattering at sulfur 32 for E_n = 7.75 MeV compared with coupled channels results.

A compilation of all relevant parameter sets used for the nuclei ^{28}Si, ^{31}P, ^{32}S is given in Table 1.

Table 1 : Parameter sets of the coupled channel analysis for the nuclei silicon 28, phosphorus 31 and sulfur 32.

Nucleus	Neutron energy	Real potential parameters			Imaginary potential parameters			Spin-orbit potential parameters			β_2 / β_4	coupling, (model)
		V	r	a	V	r	a	V	r	a		
^{28}Si	7.75	50.97	1.13	0.735	7.90	1.19	0.568	5.01	1.08	0.658	0	spherical
^{28}Si	7.58	51.5	1.15	0.663	7.57	1.33	0.60	5.94	1.02	0.68	-0.36 0.16	rot. $0^+/2^+/4^+$
		53.6	1.15	0.660	0.0	-	-	5.94	1.02	0.68	-0.36 0.16	parameters for
								2.04*	1.02	0.68		2^+ - level
^{31}P	7.75	47.67	1.20	0.626	6.50	1.07	0.497	6.00	1.20	0.74		vibr. $\frac{1}{2}^+ \vert \frac{3}{2}^+ \vert \frac{5}{2}^+$
^{32}S	7.75	53.41	1.15	0.601	5.17	1.32	0.628	8.67	1.02	0.765	0.28 (2^+)	vibr. $0^+/\ 2^+$

* imaginary spin orbit potential

References:

[1] J.W. Hammer, G. Bulski, W. Grum, W. Kratschmer, H. Postner, G. Schleußner, Nucl. Instr. a. Meth. **A244** (1986) 455.

[2] F. Fabbri, G. Reffo : CERBERO - code, manual

[3] J. Raynal, ECIS 87 - code, private communication

[4] A. Gilbert, A.G.W. Cameron : Can. J. of Phys. **43** (1965) 1446

[5] P. Moldauer : Phys.Rev. **C11** (1974)...

2. Measurement of Analyzing Power and Differential Cross Section for Manganese 55 and Cobalt 59 at E_n = 7.75 MeV.

G. Schreder, W. Grum, M. Koch, W. Weiß and J.W. Hammer

Angular distributions of analyzing power and differential cross section have been obtained for ^{55}Mn and ^{59}Co at E_n = 7.75 MeV using the SCORPION scattering facility. The evaluation of the data is still in progress.

3. Measurement of Neutron Polarization of the Reactions ^{9}Be$(\alpha,n)^{12}$C and ^{13}C$(\alpha,n)^{16}$O.

W.Weiß, W. Grum, M. Koch, G. Schreder and J.W. Hammer

Both reactions ^{9}Be$(\alpha,n)^{12}$C and ^{13}C$(\alpha,n)^{16}$O are of interest for a theoretical point of view, because the target nuclei are the simplest α-clusters plus one neutron and attempts have been made to describe the reaction mechanism. Polarization data set closer boundaries for the configurations one has to take into consideration. Moreover both reactions are of interest as neutron producing reactions with high polarization degrees in the neutron energy range of about 4 - 10 MeV.

The evaluation of the data included all necessary corrections due to normalization of different runs, background, apparative assymetries and especially the finite geometry corrections. They were done with the Monte Carlo code JANE by E. Woye [2]. Due to limited beam time and limited α-energy, measurements were made for the first time at selected α - energies and reaction angles. Figs. 1 - 4 show the final results of the experiment, the error bars originating mostly from statistical uncertainties.

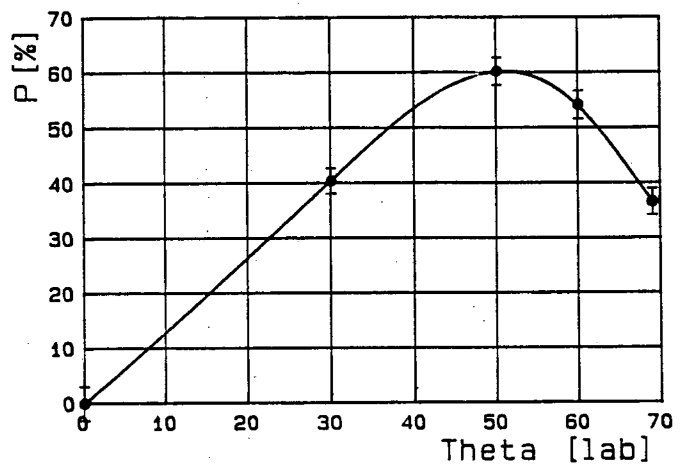

Fig. 1 Neutron - polarization of the $^{9}Be(\alpha,n)^{12}C$ reaction at E_{α} = 2.60 MeV, target-width was 70 keV. The line is only a guide for the eye.

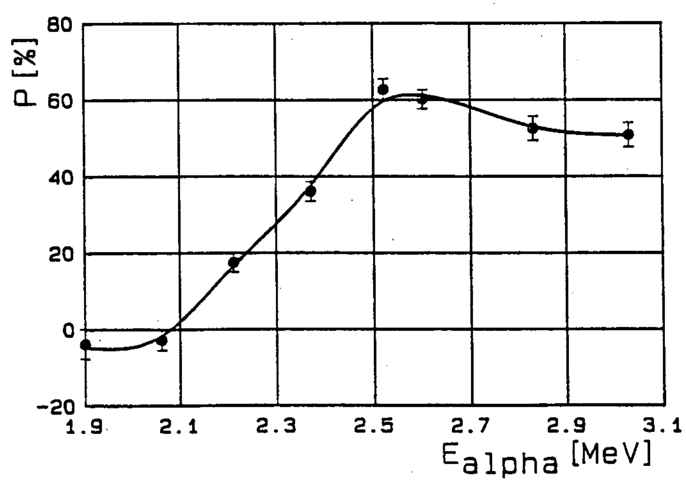

Fig. 2 Neutron-polarization of the $^{9}Be(\alpha,n)^{12}C$ reaction at a fixed reaction angle of 50 degrees (lab), target-width was 70 keV. The line is only a guide for the eye.

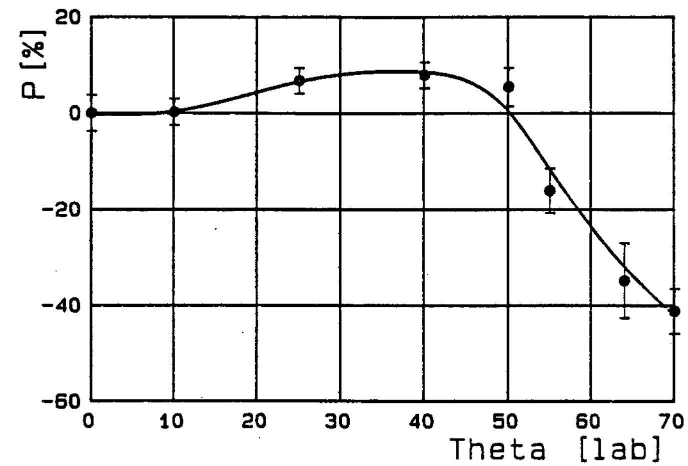

Fig. 3 Neutron-polarization of the $^{13}C(\alpha,n)^{16}O$ reaction at E_{α} = 2.406 MeV, the target width was about 55 keV. The curve serves only as guide to the eye.

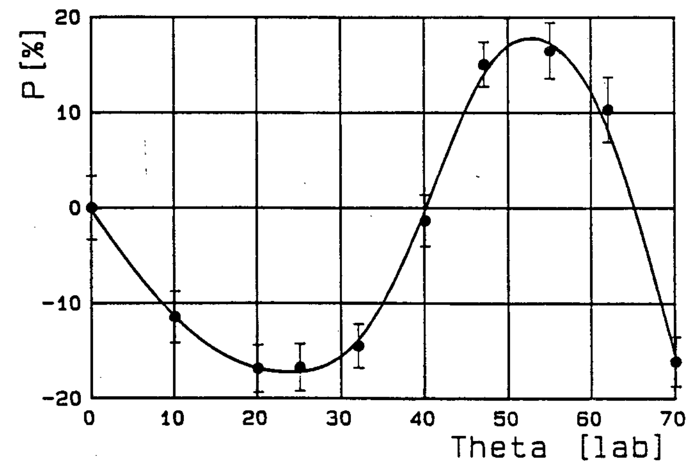

Fig. 4 Neutron-polarization of the reaction $^{13}C(\alpha,n)^{16}O$ at an α-energy of 3.308 MeV, target-width was about 45 keV. The curve is only a guide for the eye.

References :

[1] J.W. Hammer, G. Bulski, W. Grum, W. Kratschmer, H. Postner, G. Schleußner, Nucl. Instr. and Meth. A244 (1986) 455

[2] E. Woye, Thesis, Tübingen (1982)

4. Investigation of Neutron Producing Reactions in Stars: The $^{21}Ne(\alpha,n)^{24}Mg$ - Reaction.

A. Wöhr, G. Bulski, J.W. Hammer, H.W. Becker[1], H.P. Trautvetter[1], V. Harms[2], and M. Wiescher[2]

The reaction $^{21}Ne(\alpha,n)^{24}Mg$ may be involved as neutron production reaction in stars via the reaction chain :

$$^{14}N(\alpha,n)^{18}F(e^{+},\nu)^{18}O \left\{ \begin{array}{l} ^{18}O(\alpha,\gamma)^{22}Ne \\ ^{18}O(\alpha,n)^{21}Ne \end{array} \right.$$

If the (α,γ)-branch is not as dominant as assumed, depending on the temperature of the helium-burning star,the reaction $^{21}Ne(\alpha,n)^{24}Mg$ will contribute to the neutron production in stars. The neutron-production is important for the synthesis of the heavier elements with A > 56 in the s- and r- process. For the reaction $^{21}Ne(\alpha,n)^{24}Mg$ there exist only data at energies > 1.7 MeV [1], whereas the relevant energy range for helium burning is near 200 keV.

The investigation was realized in the α-energy range from 900 to 2350 keV. Several unknown resonances were found at the energies $E_{\alpha\ lab}$ = 1340, 1404, 1540, 1640 and 1740 keV. Three resonances observed by Haas and Bair [2] could be confirmed at the energies $E_{\alpha\ lab}$ = 1860, 2060, 2270 keV. After the standard unfolding procedure with the FANTI code the excitation function for the neutron groups n_0 and n_1 could be evaluated, for n_1,

---

1 Institut für Kernphysik, Universität Münster

2 Institut für Kernchemie, Universität Mainz

data. The result is shown in Fig. 1. These investigations will be continued with improved detection methods and longer measuring times to extend the observed energy range to still lower energies. It is necessary to discriminate more against the disturbing $^{13}C(\alpha,n)^{16}O$ - reaction, being always present as background.

References.

[1] H.B. Mak, D. Ashery, C.A. Barnes : Nucl.Phys. **A226** (1974) 493

[2] F.X. Haas, J.K. Bair : Phys.Rev. **C7** (1973) 2432

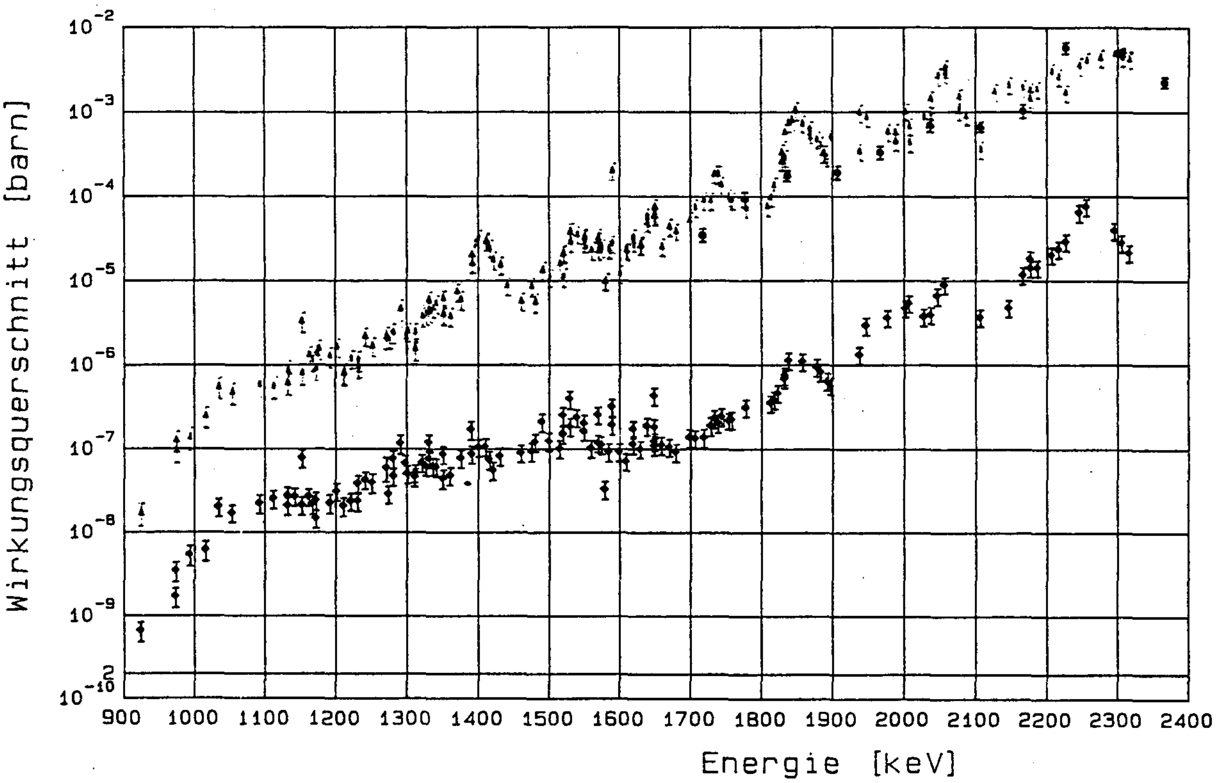

Fig.1 Excitation function of the reaction $^{21}Ne(\alpha,n)^{24}Mg$. The upper points reproduce the cross section course of the n_1-group, the lower points that of the n_0-group.

PHYSIKALISCH-TECHNISCHE BUNDESANSTALT
BRAUNSCHWEIG

1. Cross Sections

1.1 Differential Cross Section of $^{16}O(n,n)^{16}O$ between 6 MeV and 15 MeV

G. Börker, R. Böttger, H.J. Brede, H. Klein, W. Mannhart, B.R.L. Siebert

The differential cross section of the reaction $^{16}O(n,n)^{16}O$ was measured at 9 energies between 6.36 and 14.89 MeV with the PTB TOF spectrometer, using a thin-walled aluminum can containing water as a scattering sample. Extensive Monte Carlo calculations (code STREUER III) were performed in order to reduce uncertainties in the determination of the effective scattering angle, the fluence attenuation and the multiple scattering in the sample. The assumed efficiency of the NE213 detectors employed in these measurements, based on calculations with the NRESP5 code, could be

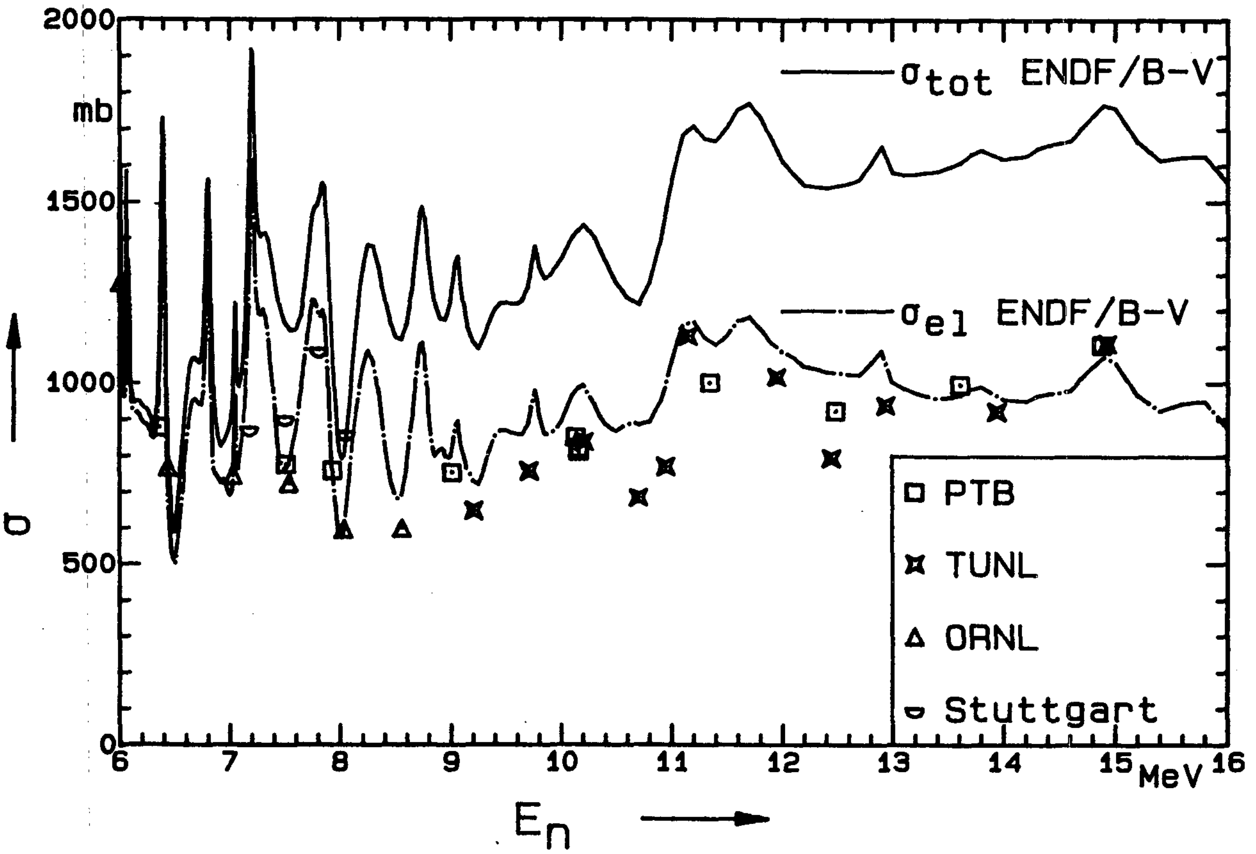

Fig. 1 Elastic neutron cross section of oxygen

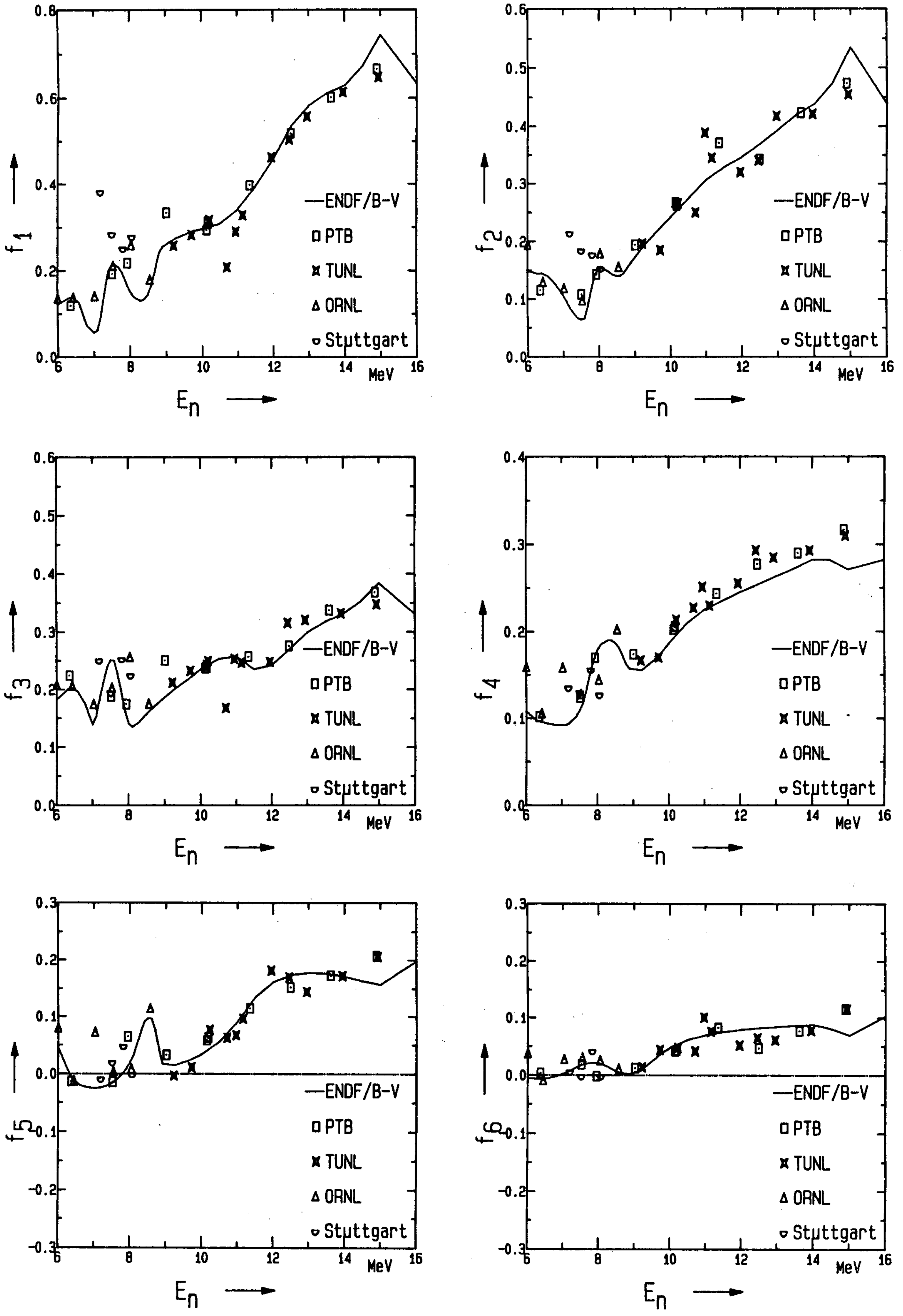

Fig. 2 Energy-dependent Legendre coefficients

verified within uncertainties of 1.5 % by the simultaneously measured n-p scattering and by comparison with a Los Alamos-type proton recoil telescope. The total and differential elastic oxygen cross sections extracted show quite large deviations from the ENDF/B-V standard data file.

The present data are plotted in Fig. 1 and are compared with ENDF/B-V and with data from the Triangle Universities Nuclear Laboratory [1], from the Oak Ridge National Laboratory [2] and from the University of Stuttgart [3]. The deduced Legendre coefficients f_1 to f_6 are shown in Fig. 2.

1.2 The Break-up Reaction D(d,np)X,Y

S. Cabral*, G. Börker, H. Klein, W. Mannhart

The energy spectra of neutrons produced by deuterons bombarding a deuterium gas target were investigated for mean projectile energies from 5.34 MeV to 13.29 MeV (in

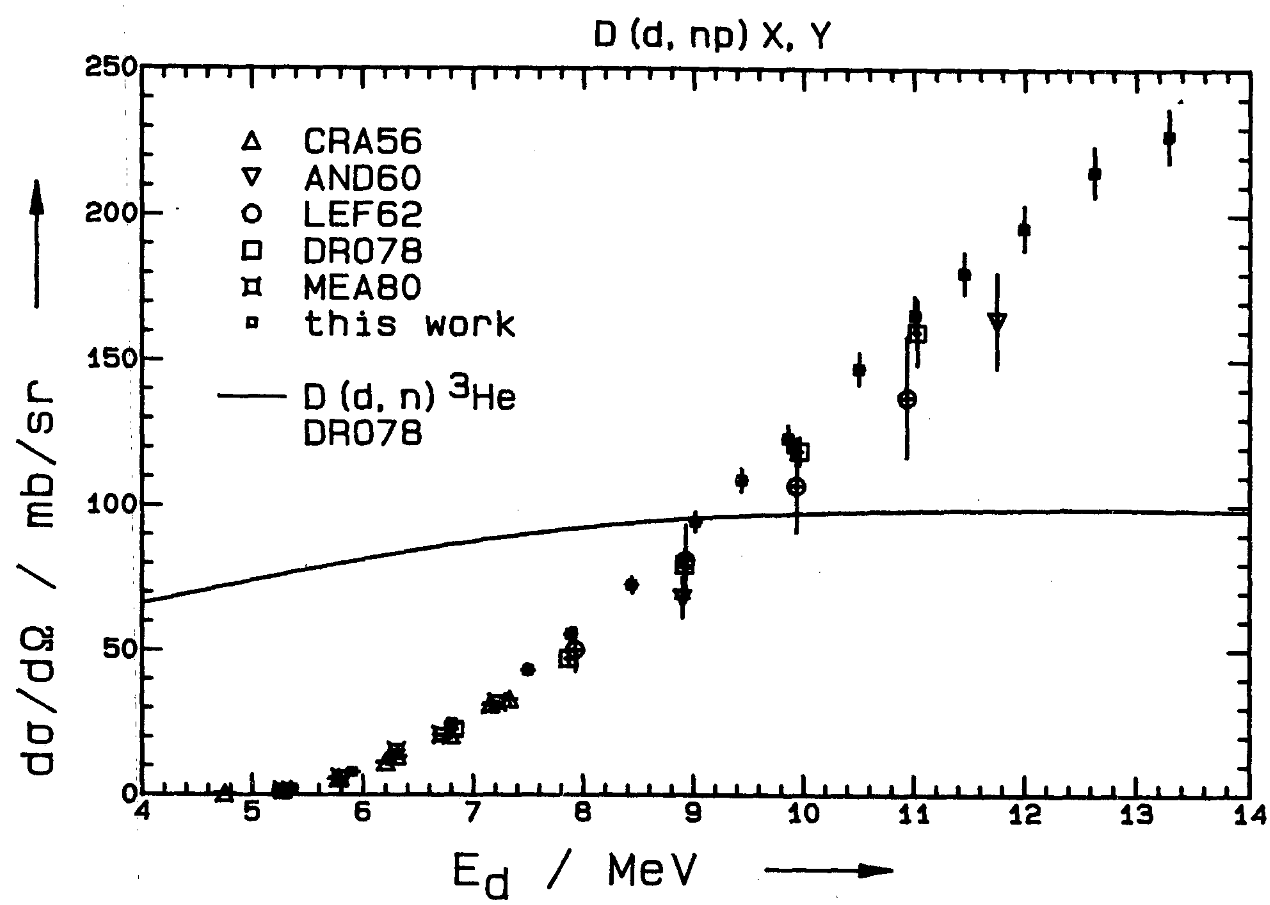

Fig. 3 Energy integrated differential zero degree break-up cross section

* Instituto Engenharia Nuclear, Rio de Janeiro, Brazil

steps of about 0.5 MeV) and for neutron emission angles between 0 degrees and 15 degrees (in steps of 2.5 degrees). The continuous energy distribution caused by deuteron break-up reactions D(n,np)X,Y, which starts at about 6.5 MeV below the mono-energetic peak from the $D(d,n)^3He$ reaction, could be analyzed for energies $E_n \geq 1.1.$ MeV. The yield was absolutely scaled with respect to the yield of the $D(d,n)^3He$ reaction as evaluated by M. Drosg [4]. The result is shown in Fig. 3 and compared with the data of other authors [4 - 8].

1.3 Neutron Activation Cross-Section Ratios between 10 MeV and 14 MeV

G. Börker, S. Cabral*, H. Klein, W. Mannhart

The production of "monoenergetic" neutrons between 10 MeV and 14 MeV with the reaction D(d,n)He-3 is accompanied by a broad energy distribution of break-up neutrons which must be corrected in activation experiments. For this purposes, the actual neutron energy distribution was measured with time-of-flight methods (see contribution 1.2). Based on these data, correction factors for various neutron activation reactions were derived. At three discrete neutron energies the relative contribution to the activation due to the break-up neutrons was calculated based on available excitation functions (ENDF/B-V). The results are listed in Table I.

These correction factors were applied in the measurement of the cross sections of Al-27(n,α), Fe-56(n,p) and Ni-58(n,p) relative to each other. Preliminary results are given in Table II. The experimental data are compared with those obtained from the Evaluated Neutron Data File (ENDF/B-V) with the exception of Al-27(n,α) where the evaluated data of Vonach et al. [9] were used. The uncertainties of the calculated ratios are based on the ENDF/B-V covariance file with relative uncertainties of more than 10 % in the case of the reaction Ni-58(n,p). The data in Table II confirm that even for large break-up neutron contributions (as for Ni-58(n,p), for example), the corrections can be properly taken into account.

Further experiments are planned such as a measurement of the Al-27(n,α) cross section relative to U-238 (n,f) with the aim of improving knowledge of the important standard cross section of Al-27(n,α) between 10 MeV and 14 MeV.

* Instituto Engenharia Nuclear, Rio de Janeiro, Brazil

Table I Contribution of break-up neutrons relative to that of the monoenergetic neutrons for various neutron induced reactions

Neutron energy (MeV)	$^{27}Al(n,\alpha)$	$^{56}Fe(n,p)$	$^{58}Ni(n,p)$	$^{238}U(n,f)$
10.43 ± 0.19[a)]	0.00 %	0.00 %	9.96 %	21.05 %
11.94 ± 0.20	0.00 %	0.15 %	50.85 %	50.24 %
13.79 ± 0.21	2.08 %	9.16 %	165.79 %	89.33 %

a) FWHM of the monoenergetic neutron peak

Table II Neutron cross section ratios

Neutron Energy (MeV)		Neutron Cross Section Ratios: $\frac{^{56}Fe(n,p)}{^{27}Al(n,\alpha)}$	$\frac{^{58}Ni(n,p)}{^{27}Al(n,\alpha)}$	$\frac{^{58}Ni(n,p)}{^{56}Fe(n,p)}$
10.43 ± 0.19	Experiment	0.835 ± 0.018	6.44 ± 0.14	7.57 ± 0.20
	Calculation	0.796 ± 0.037	6.07 ± 0.68	7.61 ± 0.89
11.94 ± 0.20	Experiment	0.887 ± 0.020	4.96 ± 0.17	5.45 ± 0.14
	Calculation	0.871 ± 0.040	4.67 ± 0.74	5.36 ± 0.86
13.79 ± 0.21	Experiment	0.933 ± 0.020	3.48 ± 0.19	-
	Calculation	0.906 ± 0.019	3.61 ± 0.64	-

2. Neutron Spectrum of Californium-252

2.1 Cf-252 Fission Neutron Spectrum above 15 MeV

R. Böttger, A. Chalupka*, L. Malik*, S. Tagesen*

In order to answer the question concerning high energy fission neutrons (E_n > 20 MeV) from Cf-252 [10 - 12] an additional time-of-flight (TOF) experiment was performed in collaboration between the PTB and IRK. The identification of neutrons from Cf-252 is a problem in this energy region because of the background from cosmic particle radiation randomly distributed in the TOF spectrum. The reduction of this background was achieved by performing the experiment in a mine, at least 600 m below ground. We found a suitable site in a mine in Bad Bleiberg (Carinthia, Austria) and measured the fission neutron spectrum in the energy range from 14 to 30 MeV with an NE213 neutron detector (25.4 cm Ø x 5.08 cm) and a fission fragment detection device (fission rate 150 000 s^{-1}) both from the PTB. A micro-processor controlled measuring and data collection system capable of withstanding the environmental conditions in this mine was developed at IRK. For the neutron detection efficiency of the scintillator in the energy range 15 MeV $\leq E_n \leq$ 20 MeV, the result of the NEFF4 calculation was used. For higher energies the efficiency was extrapolated on the basis of hydrogen cross section data only. Off line data reduction was performed for a bias of at least 4 MeV equivalent electron energy. A large part of the TOF spectrum was reserved for the determination of the randomly distributed background events between the photon peak and the upper end in the TOF spectrum. The effort of a two-month running time of the mine experiment was fully justified, as we found an extremely low background in the TOF spectra which could not have been obtained with this electronic equipment above ground. Thus the statistical uncertainty of the experimental data could be considerably reduced, particularly for neutron energies higher than 24 MeV, compared with previous experiments [10 - 12]. Comparing the data with a Maxwellian energy distribution (temperature parameter T = 1.42 MeV) we do not find any significant deviation from this common spectrum representation. This finding is in agreement with recent results of Mannhart [13] from integral measurements which do not indicate any neutron excess in the high energy part of the Cf-252 spectrum.

*Institut für Radiumforschung und Kernphysik, Vienna, Austria

2.2 Evaluation of the Cf-252 Fission Neutron Spectrum

W. Mannhart

The results of seven recent time-of-flight measurements of the Cf-252 neutron spectrum were used in the evaluation. Based on the available information, for each experiment a complete uncertainty covariance matrix was generated. The data were combined by generalized least-squares techniques. The evaluation was carried out with 70 energy grid points between 25 keV and 19.8 MeV. The individual experimental data were extrapolated to these grid points by using the shape of a Maxwellian distribution specific to each experiment. The evaluation gives a value of χ^2 per degree of freedom of approximately unity and hence does not indicate any incompatibility between the experiments. The resulting relative uncertainty of the evaluated data is smaller than 2 % between 180 keV and 9.3 MeV. The evalulated data at discrete neutron energies are plotted in Fig. 4. The error bars given were obtained from the diagonal elements of the final covariance matrix.

A comparison of these results with the theoretical descriptions available [14, 15] shows that none of these theories is compatible with the evaluated data over the whole energy range. It was therefore impossible to use a theory for the interpolation between the evaluated data at discrete neutron energies. Instead, a weighted spline interpolation was used to generate a continuous curve through the evaluated data points.

In the near future it is planned to combine additional experimental data, especially the results of integral measurements and of recent time-of-flight experiments performed at very high neutron energies, with the present evaluation. With these data a further reduction of the large uncertainties of the present evaluation above 14 MeV neutron energy is expected.

3. Radionuclide Data

3.1 Half-Lives

H. Schrader, K.F. Walz

The half-lives of the radionuclides ^{56}Co and ^{125}I were determined by following the decay of the radioactive substance with a pressurized 4π ionization chamber. A source consisted of 2 ml radioactive solution in a sealed glass ampoule. The sources

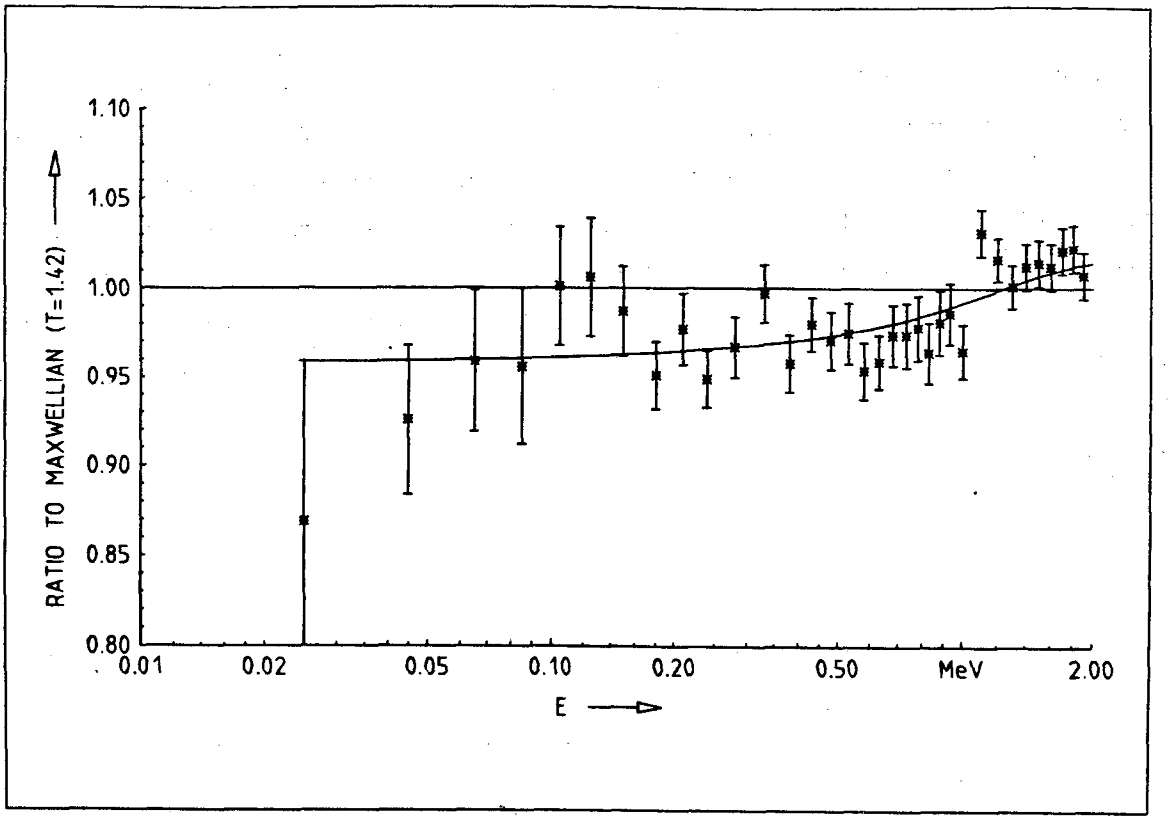

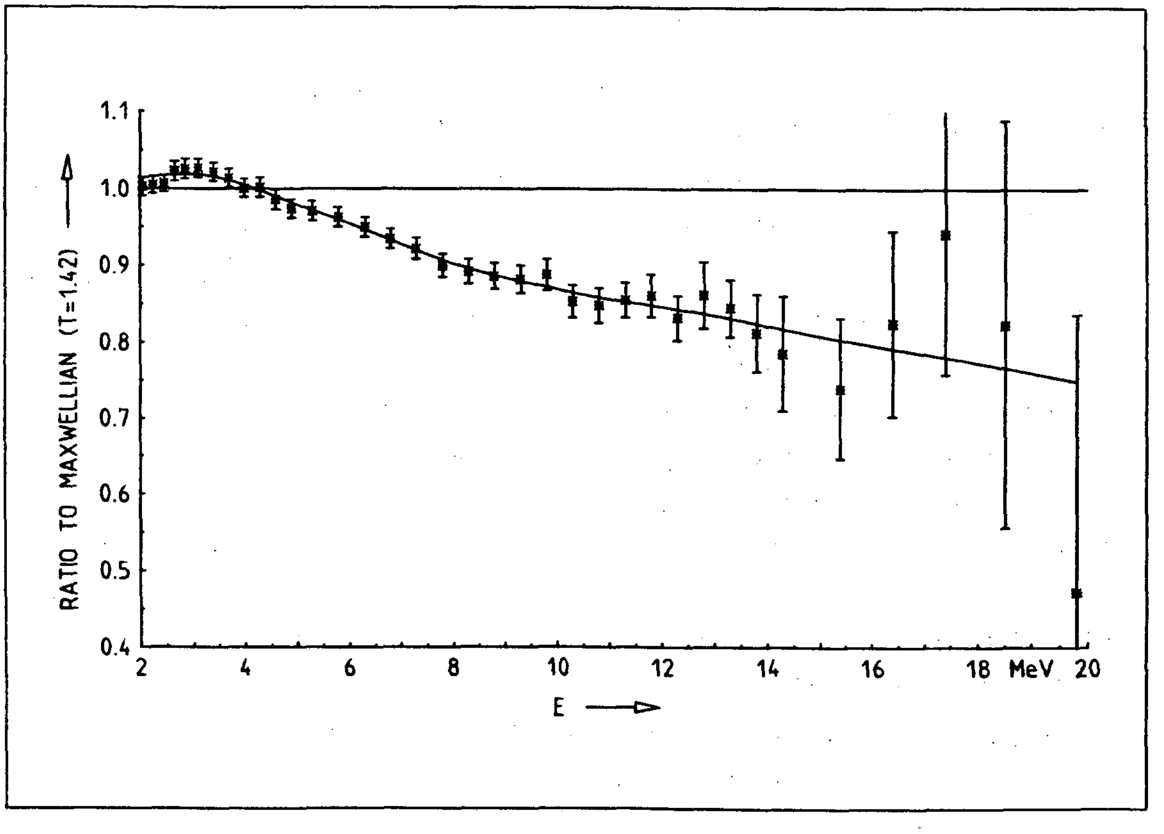

Fig. 4 Evaluated data of the energy distribution of the neutrons from Cf-252 relative to a reference Maxwellian with kT = 1.42 MeV. The continuous curve was obtained by a weighted spline interpolation between the data points at discrete neutron energies.

were examined for impurities by germanium detector measurements. The stability of the chamber was checked by measurements of a radium reference source at the beginning and at the end of each measuring cycle. The data have been evaluated by least squares fits. Details of the data evaluation and results have been published [16]. The results for the radionuclides are summarized in Table III. The given uncertainties (in parantheses) correspond to one standard deviation and include systematic uncertainties. The measuring period t is given as ratio to the half-life $T_{1/2}$.

Table III Half-lives

Nuclide	$t/T_{1/2}$	$T_{1/2}$
^{56}Co	6.7	77.28 (4) d
^{125}I	2.7	59.39 (2) d

References

[1] S.G. Glendinning et al., Nucl. Sci. Eng. 82 (1982) 393

[2] W.E. Kinney, F.G. Perey, Report ORNL-4780 (1972)

[3] G. Keilbach, Diplomarbeit, University of Stuttgart (1985) (in German)

[4] M. Drosg, Nucl. Sci. Eng. 67 (1978) 190

[5] J.D. Anderson et al. quoted in "Fast Neutron Physics" (J.B. Marion, J.L. Fowler eds.), Part I, p. 97, Interscience Publishers, New York (1960)

[6] L. Cranberg et al., Phys. Rev. 104 (1956) 1639

[7] H.W. Lefevre et al., Phys. Rev. 128 (1962) 1328

[8] J.W. Meadows, D.L. Smith, Report ANL/NDM-53 (1980)

[9] S. Tagesen, H. Vonach, Physics Data 13-3 (1981)

[10] H. Märten, D. Seeliger, B. Stobinski, Report INDC(GDR)-17/L (1982)

[11] H. Märten, D. Richter, D. Seeliger, R. Böttger, W.D. Fromm, Proc. IAEA Advisory Group Meeting on Nuclear Standard Reference Data, Geel, 12 - 16 Nov. 1984, IAEA-TECDOC-335 (1985) 310

[12] R. Böttger, W.D. Fromm, H. Klein, H. Märten, D. Richter, D. Seeliger, in "Nuclear Data for Basic and Applied Science", (P.G. Young et al., eds.), Vol. 2, p. 1471, Gordon and Breach, New York (1986)

[13] W. Mannhart, Proc. IAEA Advisory Group Meeting on Neutron Source Properties, Leningrad, 9 - 13 June, 1986, in press

[14] D.G. Madland, R.J. LaBauve, J.R. Nix, IAEA-TECDOC-335 (1985) 267

[15] H. Märten, D. Seeliger, IAEA-TECDOC-335 (1985) 255

[16] K.F. Walz, K. Debertin, H. Schrader, Int. J. Appl. Rad. Isot. 34 (1983) 1191

FACHINFORMATIONSZENTRUM ENERGIE PHYSIK MATHEMATIK GMBH

Status Report

H. Behrens, P. Luksch, H.-W. Müller

1. Data Compilations

a) The following new issues have been published in the series Physics Data:

28-2 Schwächung der Photonenstrahlung von Radionukliden.
Teil 2: Abschirmmaterial Blei
R. Dorner, H.-G. Vogt
Auflage: 275

28-3 Teil 3: Abschirmmaterial Eisen
R. Dorner H.-G. Vogt
Auflage: 275

28-4 Teil 4: Abschirmmaterial Barybeton
R. Dorner, H.-G. Vogt
Auflage: 270

28-5 Teil 5: Abschirmmaterial Normalbeton
R. Dorner, H.-G. Vogt
Auflage: 275

28-6 Teil 6: Abschirmmaterial Wasser
R. Dorner, H.-G. Vogt
Auflage: 265

b) Landolt - Börnstein
Comprehensive Index for 6th Edition 1950 - 1980 and New Series 1961 - 1985.
Prepared by Fachinformationszentrum Energie, Physik, Mathematik GmbH, Karlsruhe and Redaktion Landolt Börnstein
Springer - Verlag 1987.

2. The Evaluated Nuclear Structure Data File (ENSDF)

ENSDF is a computerfile representing the present knowledge on nuclear structure. Printed Versions are published as the well-known Nuclear Data Sheets. The file is prepared by the International Nuclear Structure and Decay Data Network, organized by the IAEA in Vienna. The Fachinformationszentrum Karlsruhe as a member of this network is evaluating data in the mass range from A = 81 to 100.
From April 1986 to March 1987 the mass chains A = 82, 83 and 99 are published and included into the ENSDF file (see References below). Evaluations of A = 88, 89, and 93 are finished or nearly finished and will be published in some months, while the evaluation of A = 85 and 86 mass chains has just started.

The online retrievable ENSDF file has been updated in October together with the MEDLIST file, which contains decay data derived from ENSDF for application purposes, such as radiation protection or nuclear engineering. 21 mass chains have been updated.
ENSDF contains now 9766 datasets, each representing the data of a special experiment or the Adopted Levels properties of a nucleon. The information is stored in 671.606 80 byte records. This is an increase of 12.3 %.
The MEDLIST file contains presently data on 2130 radionuclides stored in 86.866 records. The increase amounts 4.7 %.
The bibliographic data Nuclear Structure References (NSR) was updated in June, September and January. 3571 documents have been added, representing an increase of 3.5 %. The database contains now 104,397 documents.

References

Nuclear Data Sheets for A = 99
H.-W. Müller and D. Chmielewska
Nuclear Data Sheets 48, 663 (1986)

Nuclear Data Sheets for A = 83
J. Müller
Nuclear Data Sheets 49, 579 (1986)

Nuclear Data Sheets for A = 82
H.-W. Müller
Nuclear Data Sheets 50, 1 (1987)

APPENDIX I

Addresses of Contributing Laboratories

Institut für Kernphysik II
Director: Prof. Dr. A. Citron
Senior reporter: Dr. S. Cierjacks
Kernforschungszentrum Karlsruhe
Postfach 3640
7500 Karlsruhe

Institut für Kernphysik III
Director: Prof. Dr. G. Schatz
Senior reporter: Dr. F. Käppeler
Kernforschungszentrum Karlsruhe
Posfach 3640
7500 Karlsruhe

Institut für Neutronenphysik und Reaktortechnik
Director: Prof. Dr. G. Kessler
Senior reporter: Dr. F.H. Fröhner, Dr. B. Goel
Kernforschungszentrum Karlsruhe
Postfach 3640
7500 Karlsruhe

Institut für Chemie (1): Nuklearchemie
Director: Prof. Dr. G. Stöcklin
Senior reporter: Dr. S.M. Qaim
Kernforschungsanlage Jülich
Postfach 1913
5170 Jülich

Institut für Reaktorentwicklung
Directors: Prof. Dr. R. Hecker, Prof. Dr. R. Schulten
Senior reporter: Dr. D. Filges
Kernforschungsanlage Jülich
Postfach 1913
5170 Jülich

Institut für Physik
Directors: Prof. Dr. Bünemann, Prof. Dr. W. Michaelis
Senior reporter: Dr. R. Pepelnik
GKSS-Forschungszentrum Geesthacht
Max-Planck-Strasse
2054 Geesthacht

I. Institut für Experimentalphysik
Senior reporter: Prof. Dr. W. Scobel
Universität Hamburg
Luruper Chaussee 149
2000 Hamburg 50

Institut für Biochemie, Abteilung Nuklearchemie
Director: Prof. Dr. G. Stöcklin
Senior reporter: Dr. U. Herpers
Universität zu Köln
Zülpicher Str. 47
5000 Köln

Institut für Kernchemie
Director: Prof. Dr. G. Herrmann
Senior reporter: Prof. Dr.H.O. Denschlag
Universität Mainz
Fritz-Strassmann-Weg 2
6500 Mainz

Institut für Kernchemie
Senior reporter: Prof. Dr. P. Patzelt
Philipps-Universität Marburg
Lahnberge
3350 Marburg/Lahn

Fachbereich Physik der
Technischen Universität München
Abteilung E14, Forschungsreaktor
Head and senior reporter: Prof. Dr. L. Köster
8046 Garching/München

Institut für Kernenergetik und Energiesysteme
Director: Prof. Dr. A. Voß
Senior reporter: DP. M. Mattes
Universität Stuttgart
Pfaffenwaldring 31
7000 Stuttgart 80

Institut für Strahlenphysik
Director: Prof. Dr. K.W. Hoffmann
Senior reporter: Dr. J.W. Hammer
Universität Stuttgart
Allmandring 3
7000 Stuttgart 80

Physikalisch-Technische Bundesanstalt
Abteilung 6, Atomphysik
Director: Prof. Dr. S. Wagner
Bundesallee 100
3300 Braunschweig

Fachinformationszentrum Energie, Physik, Mathematik
Directors: Dr. W. Rittberger, E.-O. Schulze
Senior reporter: Dr. H. Behrens
Kernforschungszentrum
7514 Eggenstein-Leopoldshafen 2